Advances in Colloid and Interface Science 308 (2022) 102755

Contents lists available at ScienceDirect

Advances in Colloid and Interface Science

journal homepage: www.elsevier.com/locate/cis

Historical Perspective

A review of the advances in catalyst modification using nonthermal plasma: Process, Mechanism and Applications

Zhiping Ye [a,b,f], Liang Zhao [a], Anton Nikiforov [c], Jean-Marc Giraudon [d], Yue Chen [a], Jiade Wang [a,*], Xin Tu [e,*]

[a] College of Environment, Zhejiang University of Technology, Hangzhou 310014, China
[b] State Environmental Protection Key Laboratory of Sources and Control of Air Pollution Complex, Beijing 100084, China
[c] Department of Applied Physics, Research Unit Plasma Technology Ghent University, Ghent 9000, Belgium
[d] Univ. Lille, CNRS, Centrale Lille, ENSCL, Univ. Artois, Lille F-59000, France
[e] Department of Electrical Engineering and Electronics, University of Liverpool, Liverpool L69 3GJ, UK
[f] Department of Chemical Engineering, Sichuan University, Chengdu 610065, Sichuan, China

ARTICLE INFO

Keywords:
Nonthermal plasma
Catalyst modification
Physicochemical properties of catalysts
Plasma-catalytic processes
Application of modified catalysts

ABSTRACT

With the continuous development of catalytic processes in chemistry, biology, organic synthesis, energy generation and many other fields, the design of catalysts with novel properties has become a new paradigm in both science and industry. Nonthermal plasma has aroused extensive interest in the synthesis and modification of catalysts. An increasing number of researchers are using plasma for the modification of target catalysts, such as modifying the dispersion of active sites, regulating electronic properties, enhancing metal-support interactions, and changing the morphology. Plasma provides an alternative choice for catalysts in the modification process of oxidation, reduction, etching, coating, and doping and is especially helpful for unfavourable thermodynamic processes or heat-sensitive reactions. This review focuses on the following points: (i) the fundamentals behind the nonthermal plasma modification of catalysts; (ii) the latest research progress on the application of plasma modified catalysts; and (iii) main challenges in the field and a vision for future development.

1. Introduction

More and more researchers make efforts in the research of efficient catalyst, considering to the potential applications in industries and the huge market demands [1]. To obtain a catalyst with a high catalytic activity, high selectivity, and long-term stability, great efforts have been made to design catalysts. At present, various modification methods are being investigated, including surfactant-assisted modification [2], halogenation or chemical graft modification [3], acid-base modification [4,5], chelating agent-assisted modification [6], etc. Element doping is also a modification method; for instance, the doping of alkali metals (K, Na) can help improve the reactivity on the catalyst surface and open new low-temperature reaction pathways [7,8]. In addition, some recent advanced methods have entered the research field due to their high efficiency and non-polluting nature, including ultrasonic methods [9], microwave methods [10] and plasma methods [11].

Among them, the plasma method is one of the most promising approaches for the modifications of catalysts and, particularly, nanomaterials. Plasma is a type of ionized gas that is composed of ions, electrons, free radicals, excited molecules and neutrals. According to the gas temperature (T_g), plasma can be divided into high-temperature plasma (i.e., $T_g > 5000$ K) and low-temperature plasma (i.e., $T < 5000$ K), the latter can be divided into nonthermal plasma (NTP or cold plasma) and thermal plasma [12]. NTP is characterized by different temperature scales and energy distributions of neutrality, ions, and electrons, and plasma has a high chemical reaction activity.

Considering the type of power, plasma discharge can be divided into direct current (DC) plasmas, alternative current (AC) plasma, capacitively coupled plasmas (CCPs), inductively coupled plasmas (ICPs), microwave plasmas (MWPs), electron cyclotron resonance plasmas (ECRs), radio frequency discharge plasmas (RF) and pulse plasmas. Depending on the electrode configuration, the applied dielectric material or reactor structure, various plasmas can be generated, including glow discharge (GDPs), corona discharge, dielectric barrier discharge (DBDs), gliding arc plasmas, and many others. Their most common applications in catalyst preparation or modification involve surface

* Corresponding authors.
E-mail addresses: jdwang@zjut.edu.cn (J. Wang), Xin.Tu@liverpool.ac.uk (X. Tu).

https://doi.org/10.1016/j.cis.2022.102755
Received in revised form 5 May 2022;
Available online 16 August 2022

modification, alloying, etching, oxidation, reduction, doping, surface cleaning, template removal and activation [12,13].

A typical advantage of NTP is its low operating temperature and capability to initiate chemical reactions beyond thermodynamic limits. Nevertheless, under certain circumstances a low experimental temperature can lead to the generation of residues (e.g., undecomposed precursors, moisture), having a negative effect on catalytic reactivity. Therefore, in many cases heat treatment [14], hydrogen thermal reduction [15] or washing [16] are placed after plasma treatment. However, considering the thermal effects of plasma treatment, some have also proposed the possible replacement of the traditional calcination process using plasma [17,18]. Furthermore, it has been reported that a large number of hot spots are generated on the surface of the catalyst during the NTP process, which can increase the gas temperature and is beneficial to the activation of the catalyst [19–21]. On the other hand, compared to the NTP method, most of the current catalyst modification methods are time-consuming or complex processes that require the use of poisoning or polluting chemical reagents, while NTP mainly ionizes the gas to form a highly reactive mixture, assisting catalysts undergoing physical or chemical modifications through plasma/surface interactions and associated thermal effects [22]. Currently, an increasing amount of attention is being given to NTP modification, while the complicated mechanism of NTP modification and the lack of related in situ characterization methods limit the deep investigation of plasma processing. There are few reviews on the modification mechanism of NTP from the perspective of catalyst properties, how the physicochemical properties affect catalyst reactivity, and in view of complex plasma processes, more attention should be given to physical-chemical interactions when trying to explain why the catalytic ability has been improved after plasma treatment. Most current reviews are mainly concentrated on plasma modification aspects, such as plasma doping, etching, redox, decomposition, etc.[23], as well as the role of plasma reactive species [13]. Recently, although the focus has shifted to finding the surface properties change of the catalyst after plasma treatment [24], there is still a lack of reviews discussing the chemical properties of catalysts, an analysis of the promotion effects of an improved catalyst characterization, and the recent applications of modified catalysts by plasma.

This review will comprehensively summarize all the physicochemical property changes of catalysts before and after plasma modification and discuss the role of plasma modification processes and the possible physical-chemical interactions of NTPs. Therefore, the change in the physicochemical properties of the catalyst after NTP modification and the possible modification mechanism behind NTP treatment and some aspects of catalyst enhancement assisted by plasma, such as template removal and catalyst regeneration, are described in Section 2. Then, state-of-art investigations of catalysts modified by NTP used in the field of environmental and energy regeneration are summarized in Section 3. Finally, future challenges and the development of NTP modification methods are discussed, and visions of future developments in the field are highlighted in Section 4.

2. Nonthermal plasma (NTP) modification of catalysts

2.1. Catalytic properties modified using NTP

To optimize the key influencing factors, such as the particle size, dispersibility, metal valence, surface functional groups and morphology, and to obtain a better catalyst activity, various catalyst modification methods have emerged. Among them, nonthermal plasma (NPT) or cold plasma has been widely used in the surface treatment or modification of catalysts. The purpose of this treatment includes the generation of surface vacancies [25] and defects [26], metal doping [27] and the optimization of surface morphology [28], the increase in active sites [29], and the reformation of surface functional groups [30].

2.1.1. Dispersion

Relying on the high electron temperature (energy) of plasma, the catalyst particles can quickly be nucleated, although the growth is slow, thereby effectively reducing the particle size and improving the dispersion [12]. Moreover, the newly formed nanoparticles in the plasma are mostly negatively charged, preventing particle agglomeration and decreasing the particle size compared with the heat treatment approach [13].

It was reported that a highly efficient and stable Pt-Pd/C catalyst prepared via glow electron reduction at room temperature exhibited a fine particle size of approximately 2.6 nm and a special core-shell structure with Pt as the shell, increasing the catalytic activity by nearly 4 times [31]. The room-temperature electron reduction method mainly employed glow discharge or radio frequency discharge as the electron source to reduce the metal ions with a high valence on the surface of the catalyst at room temperature, this process includes the ionization of the gas, the adsorption and surface diffusion of energetic electrons or active particles at the metal reduction center, and the breaking of metal oxide bonds [32]. In this process, nucleation under room-temperature reduction mode is initiated by electrons or the active species generated in the plasma without thermal effects. Thus, particles nucleate quickly but grow slowly (Fig. 1) [33].

In addition, NPT can rapidly decompose precursors, changing the particle size of the catalyst. Hong and co-workers [34] used an air glow discharge for the preparation of Pt-promoted Co/TiO_2 catalysts for Fischer-Tropsch synthesis (FTS). It was determined that the plasma treatment not only effectively decomposed the cobalt precursor at low temperature in a short amount of time (1–4 h), but also that the cobalt particles (~1 nm) were uniformly dispersed on the TiO_2 support. Compared to the catalyst prepared via thermal decomposition, the supported nickel catalysts treated by DBD help to decompose the nickel precursors, resulting in a better catalytic reactivity [16,35,36]. It was revealed the carbon deposition rate increases with the increase of nickel size, fine nickel-based catalysts in hydrocarbon reforming tend to promote highly reactive carbon, resulting in speeding up the gasification or hydrogenation of atomic carbon, hence, enhancing resistance to carbon deposition [37]. El-Roz et al. successfully synthesized a highly dispersed vanadium oxide cluster on nanosized Beta (P-VO_x@Beta) [38] via the decomposition of precursor by plasma treatment. The XRD results showed that unlike the V_2O_5 phase is observed for V_2O_5@Beta prepared by hydrothermal impregnation. There was no evidence of the existence of crystalline V_2O_5 phase for VOx@Beta prepared by plasma, suggesting highly dispersion of V_2O_5. Moreover, the results of TEM-EDX exhibited small size and highly dispersed vanadium oxide clusters on nanosized zeolite using plasma treatment. Similar results were also found when preparing Ni MOF-74. The unique combination of highly chemically reactive particles and low thermal effects generated by NTP leading to rapid decomposition of organic precursors and nucleation of particles may be the key reason [39]. Fig. 2 clearly shows that with an increased Co loading, DBD plasma can effectively decompose the precursor. Compared with thermal degradation, the plasma-treated catalyst has a smaller particle size and a higher dispersibility, which may be the reason for the slight colour changes [36].

In summary, NTP exhibit the potential of high efficient decomposing catalyst precursors to optimize the preparation of small-sized and highly dispersed catalysts. Hájková and Tišler found that compared with calcination at 450 °C for 6 h, the catalyst treated with NTP for 4 s had a better catalytic reactivity [40].

2.1.2. Regulation of electronic properties

Different working gas could affect the surface valence of the catalysts. On the one hand, the active particles and electrons generated by the reducing gas will rapidly reduce the supported metal. on the other hand, the valence state of the metal support may change, leading to the formation of more active oxygen vacancies to maintain charge balance. At the same time, interactions between the created high-energy

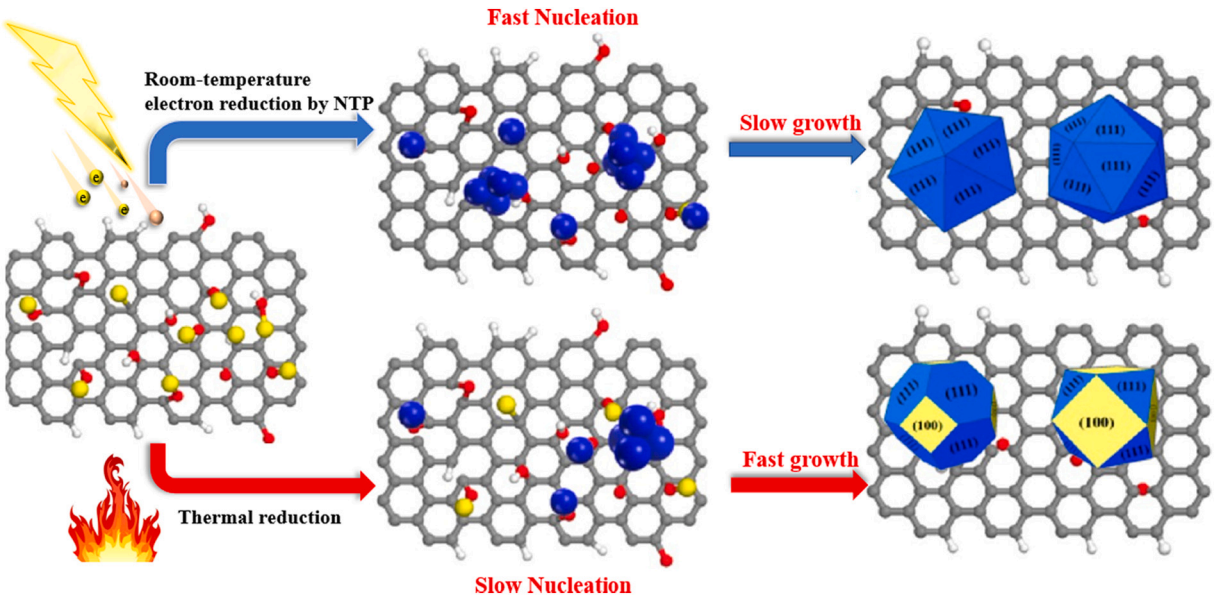

Fig. 1. Schematic diagram of nucleation and crystal growth under electron room temperature reduction and thermal reduction [33].

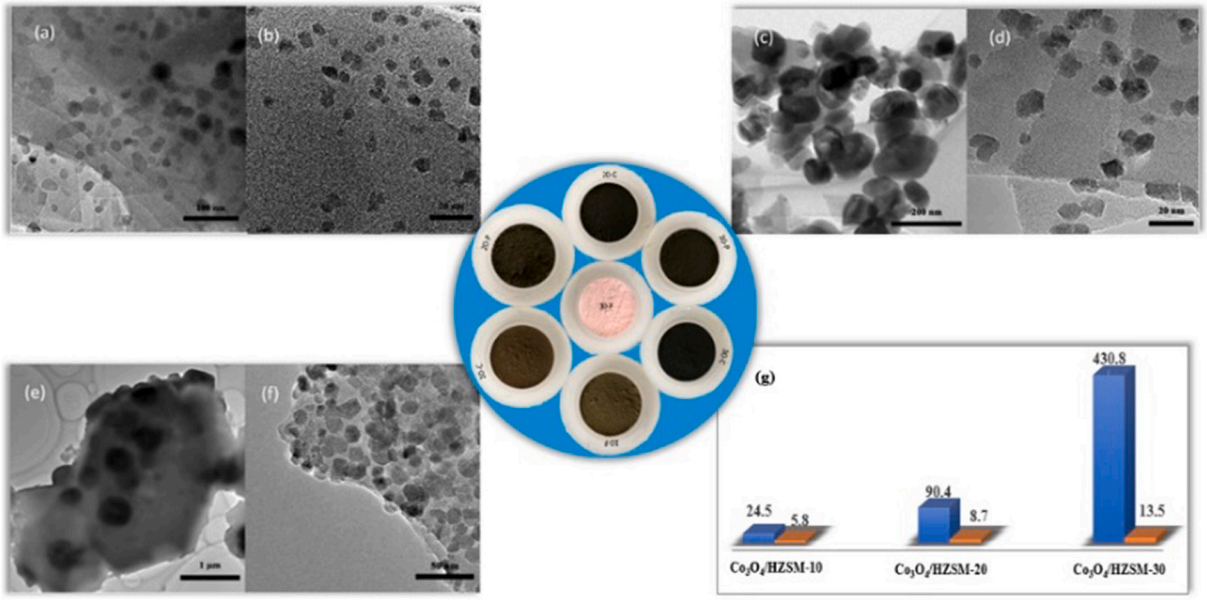

Fig. 2. TEM images of the obtained Co_3O_4/HZSM-5 catalyst (a) 10-C, (b) 10-P, (c) 20-C, (d) 20-P, (e) 30-C and (f) 30-P (C and P denote thermal calcination and NTP treatment, respectively, and the numbers stand for the Co_3O_4 loading), (g) Corresponding Co_3O_4 crystallite size (Blue is P, Orange is C), Middle: images of samples before and after calcination and plasma decomposition [36]. (For interpretation of the references to colour in this figure legend, the reader is referred to the web version of this article.)

electrons and the supported metal precursors, such as the Coulomb force, result in the enrichment of the supported metals. Di et al. [29] reported the reduction of Pd/FeO_x by plasma with a mixture of working gases of Ar and H_2, XPS analysis showed that the Pd/Fe(OH)$_x$ precursor was converted to Pd/FeO_x after plasma treatment and the content of Pd^0 on the surface increased by 16.9% compared to heat treatment. However, the oxidative gas discharge not only leads to the transition of metal valence, but also affects the content of surface oxygen vacancies. Shi et al.[41] found that O_2 plasma modified Al_2O_3 support surface increased hydroxyl radicals and decreased oxygen vacancies, which was opposite to the results of H_2 plasma treatment. Deng et al. [42] discovered an unusual feature of oxygen plasma activation when modifying the Au-based catalysts. The sample Au/TiO_2 post-treated by O_2 plasma showed a lower Au^0 content on the surface compared to traditional thermal calcination. A large amount of Au^+ was rapidly reduced to form low-coordination metal Au around the interface between Au NPs and TiO_2 support during the plasma discharge process. Ar NTP, as a mild and environmentally friendly treatment method for replacing thermal calcination and the $NaBH_4$ reduction method, can reduce Pt^{n+} to Pt^0 at room temperature (Fig. 3a and Fig. 3b). Compared to $NaBH_4$ reduction, Pt NPs treated with plasma have a smaller particle size and a higher dispersion (Fig. 3c) [43].

Moreover, NTP has a good etching and doping performance, which can further promote the generation of oxygen vacancies, the shift in the surface valence, and the change in the surface defects [44]. Xu et al. [45] reported that Ar-plasma etching of Co_3O_4 nanosheets increased the ratio

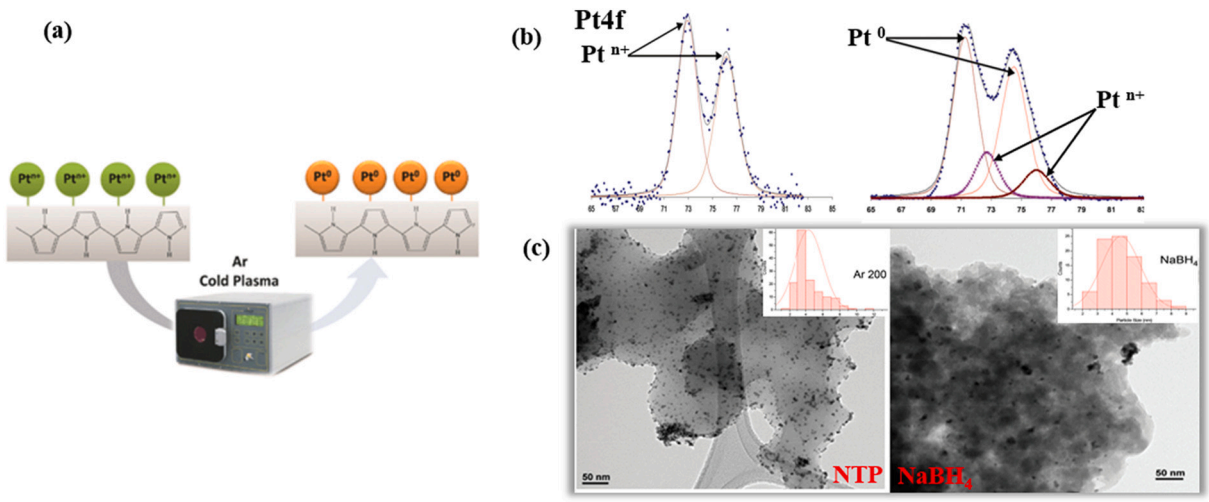

Fig. 3. (a) Schematic diagram of Pt/PPy modified by argon plasma room temperature electron reduction method; (b) XPS Pt 4f spectra of PPy impregnated with H_2PtCl_6 (left) and treated with Ar plasma at 200 W 10minx6; (c) TEM images and particle size distributions of Pt/PPy after the reduction of NTP and $NaBH_4$ [43].

of Co^{2+}/Co^{3+} from 1.0 to 1.2 on the surface, which indicated that more Co^{2+} was formed accompanied by the generation of oxygen vacancies, further enhancing NO electrocatalytic activity. Bharti et al. [25] treated Fe- and Co-doped TiO_2 films with air plasma. Increases in Ti^{3+} and oxygen vacancies were revealed in the TiO_2 band gap under plasma treatment for 60 s, leading to an increase in the absorbance and thereby improving the photochemical properties of TiO_2. Some researchers post-treated two types of doped catalysts, namely. Nitrogen-doped graphene and sulfur-doped graphene, using Argon RF plasma. The TEM (transmission electron microscope) results showed that a large number of defects were introduced on the surface of the catalyst after plasma treatment [46,47]. A facile, one-step nitrogen plasma modification strategy for the preparation of hierarchical nitrogen-doped carbon cloth (hNCC) was presented by Ouyang and his colleague [27]. Raman spectra showed that the D to G peak intensity ratio of the hNCC sample was 1.61, which is much larger than that for the untreated CC (0.93), indicating greater disorder/defects in the hNCC sample, which are important reaction sites for the formation of different nitrogen configurations [48]. An NTP etching strategy was then used to modify the Co_3O_4 nanosheets. SEM (scanning electron microscope) and TEM showed that the surface of the modified Co_3O_4 nanosheets was significantly rougher and in a discontinuous and loose state, which not only resulted in a higher surface area, but also generated more oxygen vacancies and Co^{2+} on the surface (Fig. 4) [45].

It is worth mentioning that the presence of defects on the catalyst surface was not always beneficial for catalytic reactivity. Zhu et al. [26] used glow discharge plasma for the modification of Ni/Al_2O_3 catalysts with a high proportion of dense planes. They found that fewer surface defects help to balance the formation and the gasification of carbon, hence effectively suppressing carbon deposits.

Above all, the improvement in electronic properties (oxygen vacancies, defects, and valence) of the catalyst can be achieved by plasma etching or plasma doping, thereby improving the catalytic performance. In addition, NTP modification can also change the distribution of surface elements [49]. It was revealed that the K content on the surface of the MnOx catalyst was increased from 5.7 wt% to 11.7 wt% after pretreatment via plasma etching. It was believed that the created high-energy ions, radicals, electrons and excited molecules in plasma discharge would transfer energy to surface atoms via a collision, resulting in a higher kinetic energy of the surface atoms than binding energy; thus, some atoms could be sputtered out, promoting an increase in the K content on the surface [50].

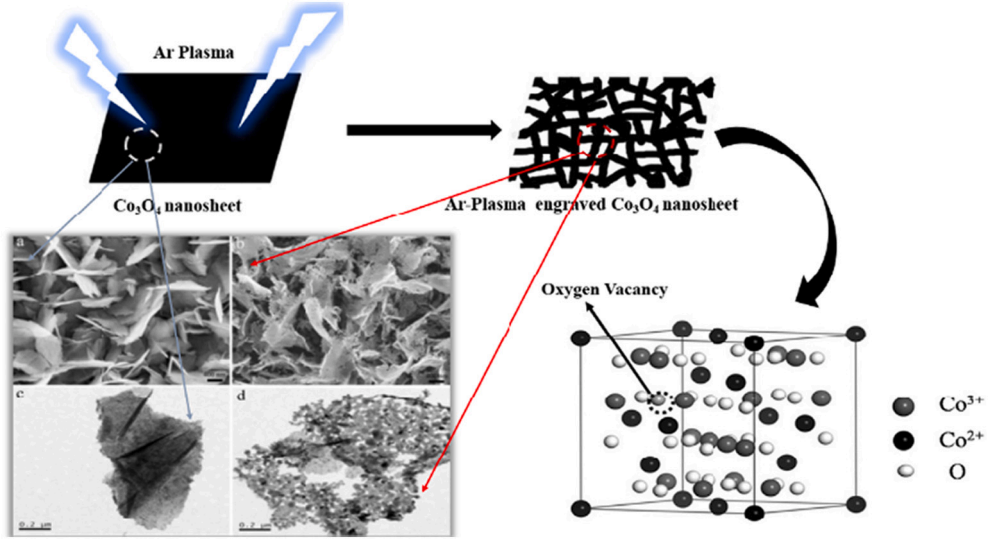

Fig. 4. Schematic diagram of Co_3O_4 modified by Ar plasma etching and SEM and TEM images of pristine Co_3O_4(ac) and Ar-plasma engraved Co_3O_4(bd) [45].

2.1.3. Surface functional groups and acid-base properties

The functional groups of catalysts affect the number of active sites and the surface properties of the catalysts [51,52]. The different atmospheres in plasma discharge bring various excited substances, which can not only act as reducing agents, as discussed above, but can also introduce chemical groups onto the surface of catalysts.

Oxygen DBD plasma was successfully applied to modify the inner surface of the one-dimensional channel of mesoporous SBA-15 particles. The plasma strongly activates the silanol groups on the channel surface, making a large number of amine groups effectively grafted in a short period of time (2 h) [30]. Recently, Kang et al. [53] achieved rapid and controllable surface modification and structural engineering of g-CN within a few minutes through an ultrafast ammonia plasma treatment. Ammonia plasma treatment could introduce amino groups on the g-CN catalyst and significantly improve the hydrophilicity of g-CN. Zhang et al. [54] and Jang et al. [55] reported the surface of a catalyst modified by a mixture of Ar and O_2 plasma. With the help of oxygen-containing radicals, alteration of the hydrophobic/hydrophilic properties of the surface was observed, thus broadening the application range of catalysts. Moreover, plasma-functionalized support materials can also promote the dispersibility of surface-supported metal particles. Loganathan [53] and Ding [56,57] proved that N_2 plasma deposition caused the formation of nitrogen-containing functional groups and a microstructure on the surface of carbon materials (Fig. 5), which made the Pt particles on the surface densely and uniformly distributed, and the particle size decreased. It was reported that the reactive ions N_2^+ generated by the plasma react with the amorphous carbon in CC and convert it into volatile CN_x. Additionally, N_2^+ with graphite carbon forms nitrogen-containing graphite microspherical particles, thereby realizing the introduction of functional groups (Fig. 6) [27].

Dameron et al. [58] determined that oxygen plasma treatment helped the formation of new oxygen-containing nucleation sites on the surface of the MWCNT array, which is a chemical foothold for the surface oxidation of Pt precursors, thereby increasing the coverage and uniformity of Pt NPs. It was reported that the CF_3 group introduced by C_2F_6 plasma affected the hydrophobicity of the carbon black support and the electronic state of the supported Pt particles [59]. An interesting phenomenon was discovered by Liu et al. [60], where graphene modified by Ar plasma not only has abundant edges and defects, but also the oxygen-containing functional groups on the surface have been greatly increased, among which the bonded oxygen content increased from 2.89% to 13.09%. This can be attributed to the edge-dangling bonds caused by NTP, which are unstable and easily absorb water or oxygen from the atmosphere.

In addition, NTP treatment will also change the acidity and alkalinity of the catalyst. Wang et al. [61] used a mixture of N_2 and H_2 DBD plasma in the modification of a series of transition metal catalysts (M/Al_2O_3, M = Fe, Ni, Cu) for the catalytic synthesis of ammonia. The results of NH_3-TPD (temperature-programmed desorption) found that the number of neutral and strong acid sites on the surface of the Ni/Al_2O_3 catalyst decreased, the number of weak acid sites highly increased after the treatment. The presence of weak acid sites on the surface can promote the formation of NH_2 intermediates, which are the most important intermediates in ammonia production [62]. Additionally, the literature shows that NTP is also an effective way to add acid sites to zeolite-based catalysts. The surface of the Pd/Al-MCM-41 catalyst was modified by Ar plasma, and NH_3-TPD showed that Brønsted acid sites and Lewis acid sites increased from 0.65 and 7.1 to 0.71 and 10.2 a.u., respectively [63].

2.1.4. Strong metal-support interaction (SMSI)

The high-energy active particles generated in plasma discharge are beneficial to generating structural defects on the surface of the material, which can help anchor the metal particles onto the support, thus improving the interaction between the metal and support via an electron transfer process [54]. This is also good for suppressing the aggregation of active components and decreasing the leaching loss of metal nanoparticles during the preparation process [64].

Brault et al. [65] reported that columnar carbon nanostructures modified by plasma not only enhance the interaction between Pt—C, but also control the size of Pt nanoparticles in the range of 1–2 nm. Zhang et al. [54] reported that Ar glow discharge plasma treatment of Au/C at room temperature can improve the catalytic stability. As revealed by TEM, compared with the H_2 thermal reduction treatment, the Au particle size on the surface after plasma modification was significantly smaller and the dispersibility was higher; moreover, metal particles were recessed into the carbon substrate after plasma treatment (Fig. 7). This may be due to the edge sputtering of carbon caused by Ar plasma, leading to carbon depression and further enhancing the anchoring effect. In addition, NTP can also be applied to improve the interactions of bimetal oxides. It was reported that the interaction between manganese oxide and cerium oxide was enhanced during the O_2/N_2 plasma treatment, and the results showed an increase in low-crystalline Mn-O-Ce and the specific surface area [66].

In addition, Pérez et al. [67] studied the effects of different modification treatment processes (Ar plasma, Ar plasma + H_2, H_2 reduction) on the catalytic performance of Pt/CeO_2 and concluded that the order of catalytic activity was Ar plasma + H_2 > Ar plasma > H_2. The XPS (X-ray photoelectron spectrometer) and TPR (temperature-programmed reduction) results showed that the content of Ce^{3+} and the electron density of Pt particles on the surface after plasma treatment were much higher than those after H_2 treatment, which was due to the charge transfer between Pt and support, suggesting that plasma treatment could enhance the interaction of Pt-CeO_2. Enhancement of the Ni-support interaction was also observed after prolonged exposure to hydrogen plasma treatment, indicating the potential of plasma reduction to be replaced with a traditional thermal treatment [68].

2.1.5. Morphological characteristics

NTP can effectively improve the morphological characteristics of the

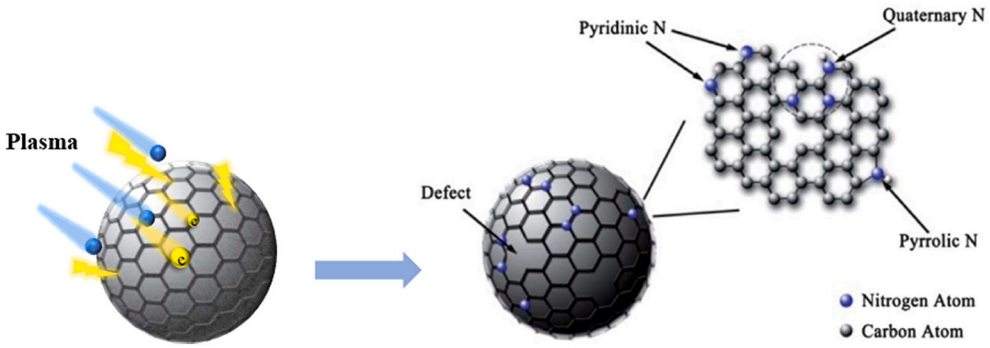

Fig. 5. (a) Schematic diagram of the preparation of doped nitrogen by Ar glow plasma [57].

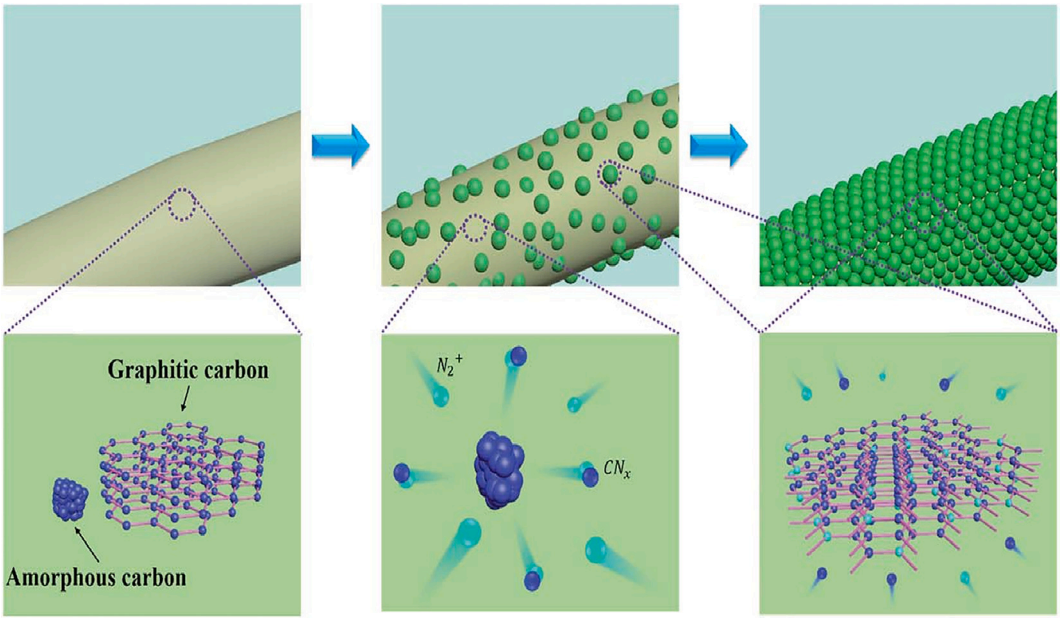

Fig. 6. A schematic formation process of the hNCC by plasma activation from the untreated CC [27].

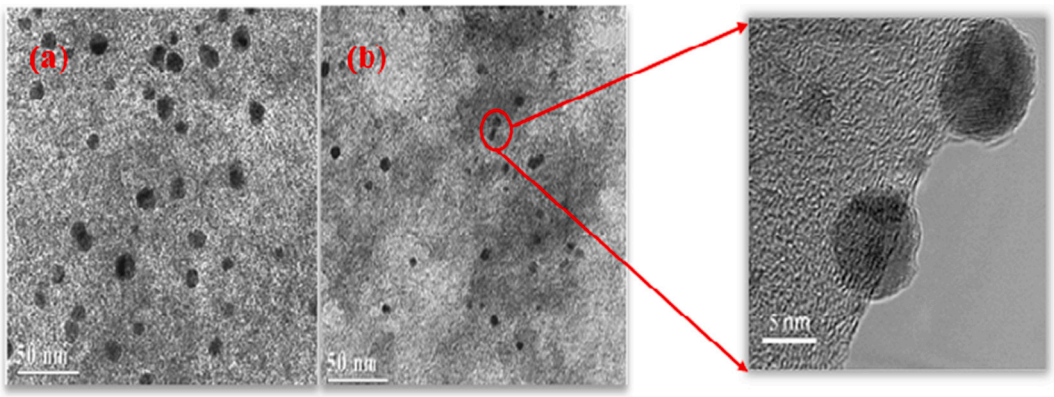

Fig. 7. TEM images of the Au/C- H (H_2-reduced) (a) and Au/C-P (b) [54].

catalyst surface, such as the pore structure, roughness, arrangement, height, and shape. Large amounts of plasma active species, such as energetic electrons, ions, radicals, etc., collide at the surface of the catalysts, providing highly controllable and selective morphology changes.

Plasma etching is an effective method that is often used to design porous structured catalysts. Low-pressure oxygen plasma was employed to oxidize the polycrystalline copper foil, and a rough surface and pore structure could be observed after treatment [69]. It was reported that Ar plasma could produce many holes with a diameter of approximately 15 nm in plasma-treated graphene, while the macrostructure remained. It was believed that this structure provided abundant active sites and retained the good conductivity of graphene [70]. It was also reported that N_2 plasma can directly convert foamed metal Ni into nickel nitride with a spatial structure, and as the treatment time increases, the interlinking structure of pores is formed [71]. Duo et al. [72] reported that graphene-supported Co_9S_8 nanoparticles (Co_9S_8/G) modified via NH_3 plasma showed that N was doped into graphene and Co_9S_8, and some nanosized holes on the graphene surface shown by TEM confirmed the etching effect of plasma.

NTP modification can also be applied for the synthesis of catalysts with the desired morphology. Xu et al. [73] proposed a one-step synthesis method of carbon nanoparticles based on plasma electrochemical technology. Crystalline platinum nanoparticles and amorphous carbon nano-carbides can be simultaneously generated to form Pt/C nanocomposites directly in plasma. Tripathi et al. [74] determined that oxygen plasma can directionally regulate the growth of carbon nanotubes by increasing the nucleation sites in CNTs, which leads to more collisions in the process of growth, thereby inhibiting the bending growth. As Fig. 8 shows, with plasma treatment, the formation of multiwalled carbon nanotube networks (MWNTs) can be observed compared to horizontal networks without plasma treatment. Yang et al. [75] reported that oxygen RF plasma treatment of a thin layer of alumina at room temperature can resist the diffusion of active component iron particles and promote the growth of carbon nanotube (CNT) forests, which causes an increase in the height of carbon nanotube forests from ~0.2 to >2 mm. Therefore, the NTP treatment of catalyst supports is potentially useful for the growth of ultrahigh-density nanotube forests, such as interconnects in integrated circuits and heat sinks.

In addition, Gao et al. [28] reported that the shape of the catalyst can be adjusted via NTP treatment. They successfully designed a nano-copper catalyst with tunable copper (100) facets using low-pressure O_2 plasma. Moafi et al. used different atmospheres as cold plasma sources to modify Ce-doped ZnO. The morphology of the Ar plasma-treated catalyst is completely transformed into nanoflowers, while after He and N_2 plasma treatment, it completely changes into nanorod structures, and the photocatalytic performance of the plasma-

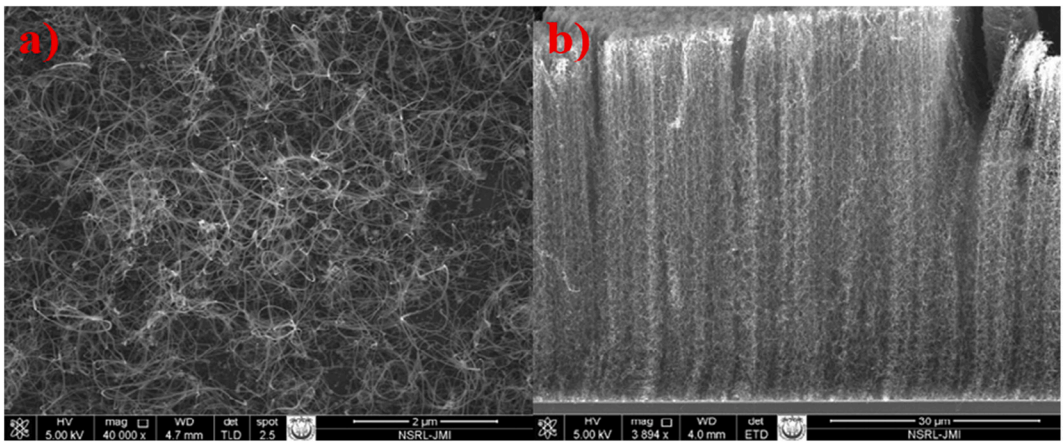

Fig. 8. FESEM images of grown CNTs: a) without plasma treatment, b) plasma treatment [74].

treated Ce-ZnO sample is effectively improved [76].

2.2. Other modifications of the catalyst via NTP

2.2.1. Removal of templates and harmful residues

Some materials, such as carbon nanotubes, polystyrene, anodized aluminium oxide membranes (AAOs) and polyvinylpyrrolidone (PVP), are frequently used as templates [77–80] for the synthesis of nanoparticles and micro/mesoporous materials [81]. However, it is difficult to clean the surface due to the close-packed layers that form narrow gaps, cavities, and curvatures with small radii [82]. Traditional effective methods for removing templates and some harmful substances (such as organic ligands, pollutants adsorbed or generated on the catalyst surface) include high-temperature calcination and acid-base treatment. However, the former is not applicable for some heat-sensitive substrates. The latter may adversely affect the structure of the catalyst, or even produce some impurities, and the use of acid-base reagents will also bring secondary pollution [83,84]. Currently, NTP, as a novel technique, has been revealed to be extremely efficient in degrading organic molecules, structure-directing agents and templates at room temperature [85].

It was proposed that the carbon removal by oxygen DBD plasma was due to the formation of micro-combustion or localized 'spot' combustion (Fig. 9a). The discharge spark was observed to be accompanied by the removal of the carbon template. This indicates reactions between oxygen species ($O(^3P)$, $O(^1D)$, O_3) and the carbon template, the process is as follows [86]:

i. Production of Ozone and Oxygen Atoms:

$$e + O_2 \rightarrow e + O(^3P) + O(^3P) \quad (1)$$

$$e + O_2 \rightarrow e + O(^1D) + O(^3P) \quad (2)$$

$$O + O_2 + M \rightarrow + M \rightarrow O_3 + M \quad (3)$$

ii. These oxygen species react with the carbon, causing micro-combustion, and the carbon template is removed:

$$ZrO_2/C + O + e \rightarrow ZrO_2 + 1/2CO_2 \quad (4)$$

$$ZrO_2/C + O_3 + e \rightarrow ZrO_2 + 1/3CO_2 \quad (5)$$

After plasma treatment, a colour fade of black ZrO_2/C particles was observed, and eventually the sample turned white (Fig. 9b), suggesting that the carbon template was successfully removed. The results showed that the obtained ZrO_2 was porous and had channels of different sizes. Meanwhile, the morphology of the sample was also affected, and N_2 sorption and XRD revealed that the prepared mesoporous ZrO_2 has a wide pore size distribution and a monoclinic crystal structure, this monoclinic lattice structure is usually obtained at calcined temperatures above 1000 °C, however, the desired catalysts also can be obtained using O_2 plasma treatment, and it was revealed the gas temperature was below 150 °C, suggesting the promoting of unfavourable thermodynamically reactions using plasma treatment [86]. Liu et al. [87] also successfully removed the molecular sieve template via air DBD plasma. They proposed that template removal was due to the dissociation of the template molecule caused by high energetic electrons and oxidation by active oxygen radicals. Thermal imaging results confirmed that the template was removed at a temperature of approximately 125 °C. This helped avoid the disadvantages of a high-temperature operation destroying the structure of molecular sieves. Compared to calcination, DBD plasma is able to preserve the structure accompanied by the removal of the framework template due to the low temperature [88]. In addition to the synthesis of micro- or mesoporous materials, NTPs can also be used to synthesize nanomaterials. It was reported that plasma discharge on the order of Ar and O_2 can be used to remove tetraethylammonium (TEA)

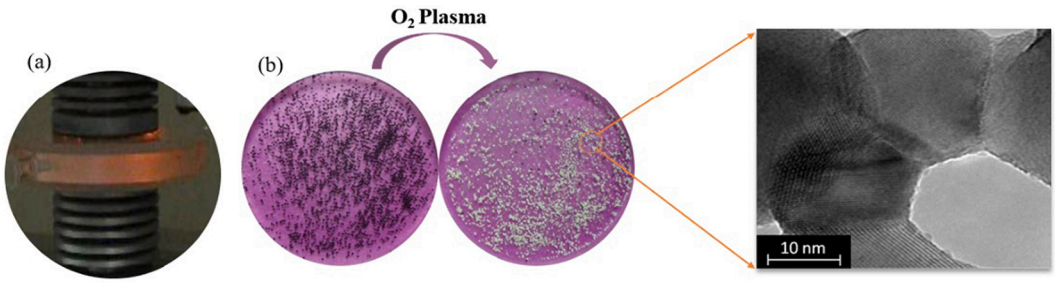

Fig. 9. (a) Micro-combustion or local "spot" combustion in the process of O_2 DBD plasma carbon removal (b) Photographs of samples before and after carbon removal and corresponding TEM images [86].

organic templates from nano-sized beta crystals in a few minutes without carbon deposition [89]. Moreover, NTP can be applied to clean the catalyst surface via the removal of contaminants and organic ligands. Non-oxidizing He plasma was employed to remove organic ligands in colloidal nanocrystals, forming all-inorganic solid films. It was determined that the ligands were degraded by excited species (e.g., He*) rather than high-energy photons. Compared with oxidizing feeding gases (e.g., O_2 and air) and highly ablative inert gases (e.g., Ar), the minimal ablative power and relative inertness of He plasma are attractive for soft material processing. Moreover, plasma can effectively overcome the shortcomings of incomplete removal of organics in traditional treatment, such as the calcination method, ligand replacement/stripping method, and the UV/ozone method [90]. Zhong et al. [91] reported that an iron-nitrogen co-doped porous carbon electrocatalyst (Fe-N/C), which was etched by air plasma for only 120 s, significantly increased the catalytic activity of redox reactions (ORRs). This is mostly due to the removal of unstable sp^3 and amorphous sp^2 carbon via plasma etching, which would expose more active catalytic FeN_4 centres and convert a small part of iron-based nanoparticles into FeN_4 species. Ferrah et al. [92] used CH_4/H_2 plasma to clean graphene prepared by chemical vapour deposition (CVD) and found that plasma not only maintains the quality and stability of graphene, but also effectively removes unnecessary residues from the preparation process. The optimized cleaning process almost recovers the original properties of quasi-freestanding graphene.

2.2.2. Catalyst regeneration

The manifestations of common deactivation mainly include carbon deposition in the process of hydrogenolysis, cracking, reforming, etc. [93,94], sintering resulted from a high reaction temperature [95,96], and poisoning caused by the loss of active sites due to impurities, such as sulfur and chloride contaminants.

Three catalyst regeneration methods have been explored for deactivated Pd/TiO_2, namely, supercritical CO_2 extraction of carbonaceous deposits, supply of ozone to the supercritical CO_2 stream, and low-temperature oxygen glow discharge treatment. Notably, carbonaceous deposits could be successfully removed using the second and third methods. However, the XPS results indicate that the surface of Pd treated with ozone or oxygen plasma is deeply oxidized. Therefore, further H_2 reduction regeneration is required [97]. Fan et al. [98] reported that pure oxygen plasma can effectively perform in situ regeneration of deactivated Au nanocatalysts in CO oxidation. However, the catalyst would be poisoned when nitrogen was introduced into the plasma discharge, especially when it contained 10% N_2. In situ FTIR detection showed that this was related to the formation of [NOy]s on the surface during the N_2/O_2 plasma regeneration process. Zhu et al. [99] found a significant promoting effect of water vapour on preventing poisoning when studying the in situ regeneration of Au/TiO_2 via atmospheric pressure air plasma. After 5 min of treatment with only 2.77 vol% water, the regeneration rate of the Au catalyst was significantly increased to 98%, compared to 29% without water. The presence of water vapour during the discharge helps to prevent the formation of NO and reacts with the inert carbonates ($[CO_3]s$) on the deactivated catalyst surface and decomposes them to CO_2, as can be seen in eq. R1:

$$[CO_3]s + [H_2O]s \rightarrow CO_2 + [OH]s \quad (R1)$$

However, Nikiforov et al. and Zhou et al. have successively found that the plasma peak current and discharge power both decrease with the increase of relative humidity [100,101]. The main reason is that water molecules are electronegative, and their presence causes a quenching effect of high-energy electrons. While, the production of energetic reactive particles such as OH radicals as well as O radicals from water dissociation can compensate for this to some extent [102]. Recently, it was discovered that the power supply of the plasma will also cause a difference in the regeneration effect. When the humidity is low, AC plasma shows a poor regeneration activity due to NO poisoning, but pulse plasma maintains a high regeneration ability under any humidity. This is mainly related to the special discharge characteristics of pulse plasma, that is, the highly centralized energy deposition. Moreover, the pulse plasma regeneration process only forms gaseous products of O_3 and nontoxic N_2O whether in dry or wet air [103].

Additionally, when the water vapour or oxygen content in the reaction environment increases beyond the threshold concentration, the metal catalyst is easily deactivated by oxidation, which can be regenerated by plasma reduction at an appropriate temperature. Kim et al. [104] used conventional thermal H_2 reduction reaction treatment and H_2 plasma to reduce and regenerate Cu-based catalysts that were deactivated by oxidation. The highest thermal reduction reaction rate was observed at a temperature of approximately 270 °C, and the temperature of plasma reduction was 238 °C. In addition, the plasma reduction significantly increases the hydrogen conversion rate and reduces the time required for complete reduction, which avoids sintering and ageing. Recently, AlQahtani et al. [105] found that DBD plasma promotes the in situ regeneration of iron sulfide catalysts in the reduction of sulfur dioxide (SO_2) to elemental sulfur. It was inferred from the XPS results that the NTP-induced hydrogenation of SO_2 in the gas phase during the reaction retained the active phase of FeS_2 on the catalyst surface and prevented its oxidation. What is more, NTP inhibited the thermal agglomeration of iron sulfide nanoparticles during the reaction.

In addition to metal-based catalysts, NTPs can also be used for the regeneration of non-metal-based catalysts. Jia et al. [106] employed DBD plasma under air or a mixture of He and O_2 to study the regeneration of coked HZSM-5. Fig. 10 clearly shows that plasma treatment can effectively remove part of the coke. The colour of the zeolite after the NTP treatment is between that of the fresh zeolite and the coked zeolite. In addition, with the change in the NTP treatment time, the EPR image changes significantly, which suggests that the active species generated by NTP can diffuse in the zeolite micropores. Comparing discharge gas effects, it was revealed that short-lived oxidizing substances, not ozone, are responsible for catalyst regeneration, and it was proposed that the active species concentration be increased by replacing N_2 with a noble gas such as He, which has a higher electron energy distribution function (EEDF), resulting in a higher ionization coefficient and therefore a higher yield of O atoms.

All in all, it is not difficult to find the role of NTP in modification of catalyst properties based on above discussion. As shown in Fig. 11, the NTP modification of catalysts can be divided into two processing: Low thermal effect and bombardment and reaction of energetic active particles.

In terms of catalyst particle size and dispersion, the low thermal effect makes particles nucleate quickly and crystals grow slowly, meanwhile, high-energy active particles also can promote the degradation of precursors through bombardment reactions. Both effects can effectively reduce the particle size of the catalyst and increases particle dispersibility. As for electronic properties (valence states, oxygen vacancies, defects), surface functional groups and metal support interactions, reductive or oxidative active radicals or electrons generated by NTP can change the valence state of the metal support or the supported metal. On the one hand, the electron transfer between supported metal and support caused by the different Fermi levels enhances the metal-support interactions. On the other hand, oxygen vacancies numbers changed to maintain the catalytic charge balance. In addition, high-energy active particles directly introduce functional groups and structural defects on the catalyst surface through bombardment reactions. Among them, the structural defects will bond with the elements (O, N etc.) in the gas phase due to their own instability. In terms of morphology, the etching effect can change the pore structure and surface roughness, and the controlled preparation of catalysts may be achieved by using plasma to increase nucleation sites or prevent the loss of active components. Lastly, the highly reactive particles produced by NTP can decompose catalyst templates and contaminants that remain on the surface, promoting catalyst cleaning and regeneration.

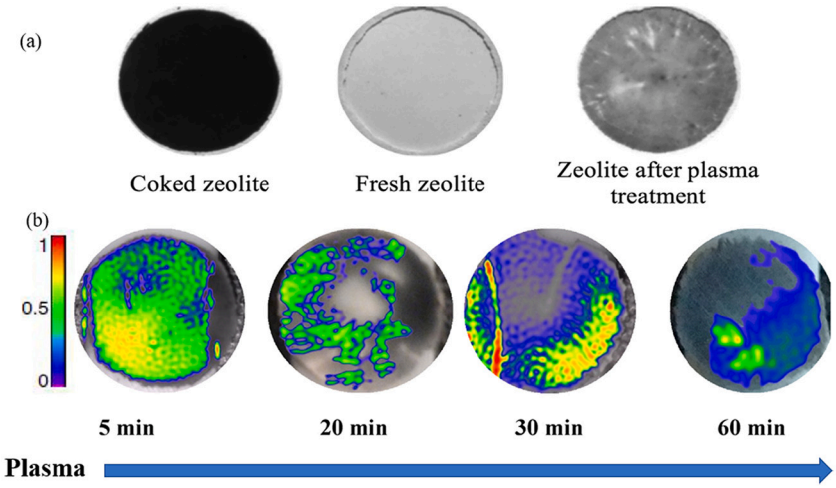

Fig. 10. (a) Images of zeolite coked catalysts, fresh catalyst and after NTP treatment. (b) 2D-EPR image with the vary of NTP processing time (the scale bar represents the spin density distribution, and the density gradually decreases from red to purple) [106]. (For interpretation of the references to colour in this figure legend, the reader is referred to the web version of this article.)

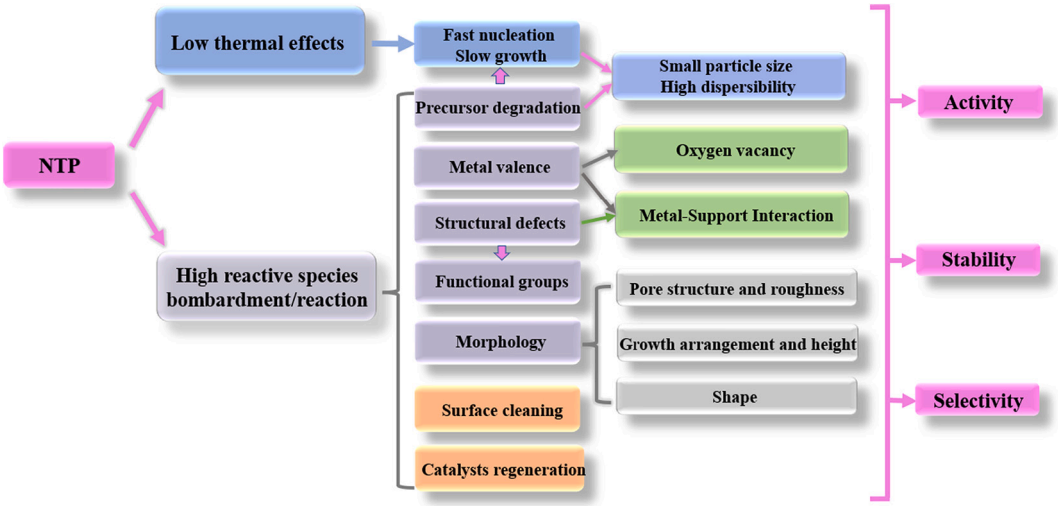

Fig. 11. Schematic diagram of the non-thermal plasma (NTP) modified catalyst mechanism.

3. The application of catalysts modified by NTP

This section will introduce the application of catalysts modified by NTP in the environment and energy fields and analyse the possible mechanism behind each process. Additionally, we will also summarize the application and performance of NTP-modified catalysts in the environment and energy fields (Table 1 and Table 2).

3.1. Atmospheric environmental

3.1.1. VOC degradation

For the photocatalyst Au/TiO_2 modified by DBD plasma under different atmospheres (O_2, H_2, and Ar), O_2 plasma-treated Au/TiO_2 exhibits the highest HCHO conversion activity (62%) under visible-light irradiation compared to the conventional calcination method (53%), the H_2 plasma-treated method (51%), and the Ar plasma-treated method (20%). It was observed that the lowest Au^0 content of the catalyst treated by O_2 plasma assisted the efficient transfer of electrons under photocatalytic degradation of HCHO [107], and the induction period of HCHO oxidation was also shortened to 1/3 of that of the calcining method [108]. Meanwhile, it was revealed that Pt/CeO_2 treated by air plasma (see Table 1) showed more oxygen vacancies and a higher dispersion of Pt NPs than Pt/CeO_2 treated by calcination. Correspondingly, the T_{90} of toluene abatement decreased from 287 °C to 208 °C, compared with the calcination method [109]. Fu et al. [110] reported that the Ru-Sn-Ti catalyst was treated with O_2 plasma, achieving a higher dichloromethane (DCM) degradation activity (T_{90}: 262 °C) in contrast to a T_{90} of 299 °C using the calcination method. It was revealed that the higher surface area, the enhanced dispersion of RuO_2 and surface oxidation of RuO_2 induced by O_2 plasma treatment were found to be the main factors determining excellent catalytic activities.

Overall, promotion effects on VOC abatement were observed when catalysts were treated with NTP prior to the application of photothermal/thermal catalytic abatement of VOCs. As mentioned above, NTP can effectively improve the surface characteristics of catalysts, such as increasing oxygen vacancies and improving the concentration and dispersion of active substances, which aid in the catalytic degradation of VOCs.

3.1.2. Denitration

As one of the main air pollutants, NO_x removal or NO_x reduction has attracted much attention from researchers [111]. The properties of NO

Table 1
Summary of the performance of NTP modified catalysts in the environmental field.

NO.	Pollutants	Catalysts	Modification conditions					Results		Ref.
			Reactor Type	Power Parameters	Gas	t (min)	Q [b] (mL/min)	Changed Characteristics	Performance	
1	HCHO	Au/TiO_2	DBD	AC [a], 5 W	O_2, Ar, H_2	5	100	• XPS: lower Au^0, more oxygen content	• (Au/TiO_2)-OP [c]: 62% • (Au/TiO_2)-HP [d]: 51% • (Au/TiO_2)-AP [e]: 20% • (Au/TiO_2)-C [f]: 53%	[107]
2	HCHO	Au/TiO_2	DBD	AC [a], 5 W,1.8 kHz	O_2	30	100	• XPS: more oxygen content and low coordination Au^0	• Au/TiO_2-OP [c] reduce the induction period to 1/3 of that of Au/TiO_2 —C [f]	[108]
3	Toluene	Pt/CeO_2	DBD	AC [a], 4.8 W, 1.77 kHz	20%H_2/N_2	180	100	• XPS: more oxygen vacancy, Pt^0 and Ce^{3+} • TEM: D_{Pt}:3.2 nm → 2.4 nm , Dispersion:40.2% → 48.9% • BET: 90.02m^2g^{-1} → 99.31 m^2 g^{-1}	T_{100} of Toluene removal • Pt/CeO_2-PT [g]: 205 °C • Pt/CeO_2-TP [h]: 175 °C • Pt/CeO_2-C [f]:135 °C	[160]
4	Toluene	Pt/CeO_2	DBD	AC [a], 1.8kHz, 4.8 W	20%O_2/ 80%N_2	30	100	• BET: 82.1 m^2g^{-1} → 87.1 m^2 g^{-1} • XPS: more oxygen vacancy, Ce^{3+}, metal support interactions • TEM: D_{Pt}:34 nm → 3.3 nm, Dispersion:33.66% → 34.38%	• T_{90} reduced from 287 to 208 °C • TOF_{Pt} = 9.88*10–4 s^{-1}, TOFov = 9.49 *10^{-5} s^{-1} • Low activation energy (63.8KJmol^{-1}) • Good stability and moisture	[109]
5	Toluene	Pd/SiO_2	DBD	3.6 W	H2	60	30	• TEM: D_{Pd}:12.8 nm → 5.1 nm, dispersion increasing	• Pd/SiO_2-P [i]: T_{98} 170 °C, Pd/SiO_2-R [j]: T_{98} 200 °C	[161]
6	Dichloromethane (DCM)	RuO_2/ $Sn_{0.2}Ti_{0.8}O_2$	DBD	9 kHz, 10 kV, 100 W	20% O_2/ 80% air	90	/	• XPS: more Pd^0 • BET:46.807 m^2g^{-1} → 37.397 m^2 g^{-1} • TEM: dispersion increasing • XPS: more oxygen vacancy and Ru^{5+} • SEM: reduce surface impurities	• $(RuO_2/Sn_{0.2}Ti_{0.8}O_2)$-P [i]: T_{90} is 262 °C • Good stability without perceptible deactivation for 24 h at 250 and 275 °C	[110]
7	NO	$LaMnO_3$/ CeO_2	GDP	AC [a], 1.5 kV	Ar	45	/	• BET: 25.185 m^2g^{-1} → 39.497 m^2 g^{-1} • TEM: dispersion increasing • SEM: particle size decreasing	• Conversions of NO and CO: 41.19 and 49.11% • High stability: 30 h	[162]
8	NO	MnCeOx	DBD	AC [a], 9kHZ, 10KV, 185 W	5, 10, 20, 60%O_2/N_2	90	/	• BET: 68.89 → 101.4m^2g^{-1}, pore volume: 0.131 → 0.286cm^3g^{-1}, pore diameter: 6.78 → 12.5 nm • XPS: Mn/Ce and Ce^{3+}/Ce increasing, more adsorbed oxygen, enhance metal support interactions, formed a low crystalline Mn-O-Ce phase	• MnCeOx-C [f]: 53% • MnCeOx-P [i] (10%): 80.5% at 275 °C	[115]
9	NO	Mn-CoOx	DBD	5,6,7,8.5KV	N_2	30, 60, 120	100	• BET: 254 → 327m^2g^{-1}, pore volume 0.211 → 0.275cm^3g^{-1} • XPS: Co^{2+}/Co^{3+} and Mn^{4+}/Mn^{3+} increasing	• Mn-CoOx-P [i]: 83.7% at 150 °C	[113]
10	CO	Au/TiO_2	DBD	25, 29, 35 kV	O_2	1, 2, 4	/	• XPS: more Au^0 species, fewer oxygen species	• CO conversion: Au/TiO_2-29 kV-1 min: 1.42 times as that of the Au/TiO_2 without plasma treatment at 30 °C	[120]
11	CO	Au/TiO_2	DBD	AC [a], 5 W, 1.8 kHz	O_2, Ar	30	100	• XPS: more O, low-coordinated Au^0	• The CO chemisorption capacity: OP [c] > AP [e] > C200 [f]	[42]
12	CO	Au/TiO_2	DBD	AC [a], 2kHZ, 7 W	O_2	30	/	• XPS: more low-coordinated Au^0, Hydroxyl • TEM: D_{Au}: 3.4 → 2.6 nm; dispersion increasing	CO conversion of Au/ TiO_2-P [i] • Au/TiO_2-P [i]:42% • Au/TiO_2-C [f]: 23.4%	[55]
13	CO	Pd/Al_2O_3	DBD	AC [a], 13.6 kHz, 19.2 kV	Ethanol-Ar	10	100	• XPS: more Pd^0 and active chemisorbed oxygen species • SEM: remove the residual carbon species	• Pd/Al_2O_3-EAP [k]: T_{100} at 130 °C • Pd/Al_2O_3-HP [d]: T_{100} at145°C	[163]
14	CO	2.0wt%Pd/ FeOx	DBD	36 kV,14.1 kHz	Ar + 50%H_2	6	100	• XPS: rich Pd species, the larger pore size of support, more Pd^0 and oxygen vacancy content	• The reaction rate of the Pd/FeOx-P [i] catalyst at 25 °C is 1.3 times that of the conventional method	[29]

a AC: Alternate current; *b* Q: Gas flow; *c* OP: O_2 Plasma; *d* HP: H_2 Plasma; *e* AP: Ar Plasma; *f* C: Calcination; *g* PT: Plasma plus Thermal treatment; *h* TP: Thermal plus Plasma treatment; *i* P: Plasma; *j* R: H_2 reduction; *k* EAP: Ethanol-Ar Plasma.

Table 2
Summary of the performance of NTP modified catalysts in the energy field.

NO.	Reaction	Catalysts	Modification Conditions						Results		Ref.
			Reactor Type	Power Parameters	Discharge gap	Gas	Q [a] (mL/min)	t (min)	Changed Characteristics	Performance	
1	Methan ation of COx	Ni/Ce/SBA-15	DBD	AC [b], 40 kV	30 mm	Ar	20	4	• SEM: Ordered Mesoporous Structure • TEM: 13.9 → 8.9 nm	• CO_2 Conversion: 79.8%, CH_4 Yield: 80% at 450 °C • CO Conversion: 97%, CH_4 Yield: 90% at 450 °C • Stability: 650 °C 30 h	[133]
2	Methanation of CO_2	Ni/TiO_2	DBD	AC[b],14KV, 200 W	8 mm	Air	/	60	• TEM: smaller Ni size • XRD: Ni (111) as the principal exposing facet	• CO_2 Conversion: 73.2% at 350 °C	[16]
3	Methanation of CO_2	Ni/$MgAl_2O_4$	DBD	14 kV, 200 W	8 mm	Air	/	90	• TEM: smaller Ni size, high dispersion • XPS: enhance Ni-support interaction	• CO_2 Conversion and CH_4 Selectivity: 90% at 350 °C	[164]
4	Methanation of CO	Ni/SiO_2	DBD	22kHZ, 14 kV	8 mm	Air	/	90	• TEM:20.2 nm–7.5 nm • XRD: crystal size of NiO: 17.3–11.9 nm, pore diameters: 6.5–9.7 nm and high dispersion • BET: 231-233 $m^2\ g^{-1}$	• 10Ni/Si-P [c]: CO Conversion: 79% at 340 °C, CH_4 Selectivity: 70% • 10Ni/Si-C [d]: CO Conversion: 32.5%	[165]
5	Methanation of CO	Ni/CeO_2	DBD	200 W, 22kHZ, 14 kV	2.5 mm	Air	/	/	• XPS: enhance interaction between Ni and Ce • TEM: highly dispersion and smaller Ni size	CO Conversion & CH_4 Selectivity: • Ni/CeO_2-P [c]:96.8% at 250 °C, 100% at 300 °C • Ni/CeO_2-C [d]:14.7% at 250 °C	[138]
6	CO_2 Electroreduction to Ethylene	Cu foil	/	20 W, 100 W	/	O_2, $O_2 + H_2$	/	14	• XPS: Cu^+ exist and stable • SEM: improved roughness and porosity	• Decrease overpotential • Ethylene Selectivity: 60%	[122]
7	CO_2 Electrocatalytic to Hydrocarbon	Cu nanocube	/	20 W	/	O_2/H_2/Ar	/	O_2(0.3)/ H_2(4–20)/Ar (5–15)	• SEM: high roughness • XPS: more oxygen content and defect sites • XRD: form Cu (100) facets	• Reduced overpotential • (Faraday efficiency) $_{max}$ of C2-C3 products:73%	[28]
8	CO_2 Electrocatalytic to CO	Ag foil	/	20 W	/	H_2/Ar/ O_2	/	O_2 (2)/ H_2 (10)/Ar(10)	• SEM: high roughness, porosity and defects • XPS: more oxygen content	• Ag-OP [e]: Faradaic efficiency towards CO at @0.6 V versus RHE: 90%	[124]
9	CO_2 Electroreduction	Dendritic Cu/Ag Dendritic Cu/Pt	/	20 W	/	O_2	/	1/5	• SEM: increase surface roughness	• Faradaic efficiency of C2-C3 products: ~ 45%	[123]
10	Methane Steam Reforming	$Ni/LaFeO_3$	DBD	100 V, 1A	8 mm	10% H_2/ Ar	50	180	• XPS: enhance the interaction between Ni and the $LaFeO_3$ supports • XRD: improved Ni dispersion	CH_4 Conversion & H_2 yield at 800 °C: • $Ni/LaFeO_3$-GNC-P [f]: 80%, 80% • $Ni/LaFeO_3$-SN-P [g]: 78%,74% Ni/ $LaFeO_3$-CP-P [h]: 69%, 70%	[166]
11	Glycerol Steam Reforming	Ni/CeO_2	GDP	150 V, 500 W, 1.125 kW	/	Air	/	120	• H_2 chemisorption: enhanced the nickel dispersion • XPS: improved the Ni—Ce interaction, form Ni-O-Ce composite • XRD: enhance the dispersion of CuO (111) crystallite plate • FESEM: best surficial morphology	• Glycerol conversion: Ni-N/CeO_2:100% at 450 °C in 8 h • Products selectivity: H_2:44.7%, CO_2:44.8%, CO:54.6%, CH_4: 0.6%	[148]
12	Methanol Steam Reforming	CuO/ZnO/Al_2O_3	GDP	DC [b], 1000 V	/	Ar	20	45		• Methanol conversion& CO selectivity: CuO/ZnO/Al_2O_3-P 95% at 240 °C, as low as 0.24%	[149]
13	ORR [i], OE R [j]	Co_9S_8/G	RF	200 W	/	NH_3	/	60	• XPS: nitrogen doping into both Co_9S_8 and graphene • TEM: exist partially etch the surface of both Co_9S_8 and graphene • Raman: increase the defect level of carbon materials	N-Co_9S_8/G: • ORR [i] result: a similar onset potential and current density to the commercial Pt/C	[72]

(*continued on next page*)

Table 2 (*continued*)

NO.	Reaction	Catalysts	Modification Conditions						Results		Ref.
			Reactor Type	Power Parameters	Discharge gap	Gas	Q [a] (mL/min)	t (min)	Changed Characteristics	Performance	
14	ORR [i]	CNTs	/	100 W, 40 kHz	/	O_2	/	0–30	• SEM: generate more defects • Raman: I_D/I_G from 0.012 to 0.157 in SWCNT and from 0.895 to 1.22 in MWCNT • XPS: more oxygen content	• OER [j] activity: overpotential: only 0.409 V at the current density of 10 mA cm^{-2} • The double-layer capacitances: SWCNT & MWCNT: 1422 μF & 1190 μF, 1.32 and 1.60 times higher than the original SWCNT and MWCNT	[158]
15	OER [j]	Co-MOF-74	RF	100 W	/	Ar, H_2	/	0–4	• FT-EXAFS: form engraved coordinatively unsaturated metal sites with more defects	OER[j] activity: • Co-MOF-HP[e]: overpotential: 337 mV at 15 mA cm^{-2}, turnover frequency: 0.0219 s^{-1}, mass activity: 54.3 A g^{-1} • Co-MOF-AP[e]: overpotential: 354 mV at 15 mA cm^{-2} • MOF: overpotential: 383 mV at 15 mA cm^{-2}	[153]
16	OER [j]	Co_3O_4	RF	100 W,13.56 MHz	/	Ar	/	0, 1, 2, 3, 4	• BET:95.27 m^2 g^{-1} → 160.26 m^2 g^{-1} • XPS: more Co^{2+} and oxygen vacancy • SEM: more defects	• The specific activity: 0.055 $mAcm^{-2}_{BET}$ at 1.6 V, 10 times higher than that of pristine Co_3O_4	[45]
17	HER [k]	NiMoN/C	RF	250 W, 13.56 MHz	/	N_2	100	15	• SEM: high roughness factor (1050) • TEM: exist porous structure and lattice fringes with an interplanar distance of 0.246 nm • XRD/XPS/EDX: exist a metal nitride material and NiMoN phase	• NiMoN-P [c]: low overpotential around 109 mV at 10 mA cm^{-2}	[156]
18	OER [k]	CoN	RF	300 W,13.56 MHz	/	N_2	/	0.5, 1, 3	• TEM: surface rougher • XPS: exist N1s peak • XRD: exist CoN phase	CoN-P [c]: • Low overpotential: 290 mV at 10 mA cm^{-2} • Durability: over 30 h in an alkaline electrolyte	[157]
19	HER [l]	Pt/C	RF	80 W, 13.56 MHz	/	N_2, Ar, Air	20	60, 180, 240	• XPS: introduce N and N, O atoms respectively • XRD: increased particle dispersion	Pt/C-AP [e]: • High TOF of ~13 H_2 s^{-1} at 40 mV • Mass activity: 7.41 A mg^{-1} Pt, 26.5 times of commercial Pt/C catalyst	[159]

a Q: Gas flow; *b* AC: Alternate current, DC: Direct current; *c* P: Plasma; *d* C: Calcination; *e* OP: O_2 Plasma, HP: H_2 Plasma, AP: Ar Plasma; *f* GNC-P: catalysts treated by Glycine– Nitrate Combustion Method and modified by plasma; *g* catalysts treated by Sol–Gel Method and modified by plasma; *h* CP-P: catalysts treated by Co-precipitation Method and modified by plasma; *i* ORR: Oxygen Reduction Reaction; *j* OER: Oxygen Evolution Reaction; *k:* HER: Hydrogen Evolution Reaction.

oxidation catalysts, such as oxygen species, acid-base sites, redox properties, and adsorption ability, are the keys for the denitration process [112].

Tang et al. [113] reported that an Mn-CoO_x catalyst modified by N_2 DBD plasma exhibited the best catalytic oxidation activity of NO conversion efficiency from 35% (over Mn-CoO_x without plasma treatment) to 83.7% at 150 °C. It was observed that the concentrations of O atoms, Mn^{4+} and Co^{2+} on the surface of Mn-CoO_x were significantly increased after plasma treatment, which were the key to NO oxidation. Zhang et al. [114] proposed that the discharge power, treatment time, and airflow of O_2 gas during plasma treatment would increase the basic functional groups, thereby improving the denitration activity. It was revealed that the removal efficiency of NO of plasma-modified catalyst reaches 95% within 1 min under the conditions of 60 W power, a treatment time of 20 min, and an air flow of 40 ml/min. The effects of discharge atmospheres (O_2/N_2: 5:95, 10:90, 20:80, 60:40, 100:1) of the plasma discharge on $MnCeO_x$ catalysts were also evaluated for NO conversion into NO_2, which is an important prerequisite step of NO_x removal. Among them, 10% O_2/N_2 plasma-treated $MnCeO_x$ showed an excellent activity with the conversion rate exceeding 80% in the temperature range of 275–325 °C compared to O_2 plasma and calcination treatment (both 53% at 275 °C). The lower oxygen in the carrier gas could prevent catalyst sintering by slowing down the reaction between the precursor and the active materials, forming a low-crystalline Mn-O-Ce phase with a higher oxygen mobility [115]. Moreover, the specific surface area of NiO-TiO_2-Al_2O_3 was revealed to increase, and the nickel particles were dispersed more evenly after the air plasma treatment, enhancing the adsorption ability of NO_x. Therefore, the NO_x conversion was significantly increased from 12% to 70% [116,117]. Similarly, Huang et al. [118] found that the NO conversion rate of O_2 plasma-treated VACF (viscose-based activated carbon fibre loaded with vanadium) (>55%) was much higher than that without the plasma treatment (<35%), which was mainly attributed to the introduction of more oxygen functional groups by the plasma, improving the dispersibility of vanadium.

3.1.3. CO removal

A dendrimer-derived Pt/Al_2O_3 catalyst activated by O_2 plasma to oxidize CO was studied by Nazarpoor et al. [119], and they observed that the O_2 plasma treatment not only removes the dendrimers covering the catalyst surface, but also obtains small-sized (2 nm) and highly dispersed Pt particles; thus, the T_{100} of CO abatement obviously decreases from 370 °C (over fresh catalysts) to 250 °C. Deng et al. found that the plasma activation of Au/TiO_2 for CO photocatalysis is closely related to the gas composition of plasma. The O_2 plasma treatment increased the surface oxygen content, which promoted superoxide (O_2^-) formation by local surface plasmon resonance (LSPR) of Au NPs. Thus, Au/TiO_2 treated with O_2 plasma has a higher CO conversion than Ar plasma and calcination treatment under the same conditions (13–14 °C), corresponding to 78%, 25%, and 60% [42]. Moreover, it was reported that the appropriate discharge voltage and discharge time were not only sufficient to decompose the gold species formed by the modified impregnation process to form metallic gold species, but also to retain many active hydroxyl groups [120]. Different posttreatment methods have a great influence on the Pd/C catalyst reduced by plasma, and the T_{100} of CO conversation decreased from 180 °C to 105 °C, corresponding to the posttreatment of H_2 calcination and deionized water washing. This high performance may be attributed to the treatment of plasma and calcination, which can completely remove the residual Cl^- ions and obtain an increasing number of metal Pd nanoparticles without aggregation [121]. Therefore, the reasonable combination of plasma and different processes can produce a certain synergy and effectively improve the catalytic effect.

3.2. Energy field

To reduce dependence on fossil fuels, catalysts are used to convert COx, hydrocarbons, and other substances into liquid fuels or gaseous energy, including CO_2 reduction and methanation, and steam. In addition, energy conversion and storage have also received widespread attention, such as the hydrogen evolution reaction (HER), oxygen evolution reaction (OER), and oxygen reduction reaction (ORR).

3.2.1. CO_2 reduction

It was reported that O_2 plasma treatment was able to rapidly oxidize copper foil to develop a stable oxide layer with a rough surface, which could reduce the overvoltage of CO_2 electroreduction and increase the selectivity towards ethylene (60%) [122]. Scholten et al. [123] also proposed that O_2 plasma treatment can effectively change the surface roughness of dendritic Cu catalysts, which helps to increase the geometric current density of the catalyst. Moreover, compared with Cu/Pt, Ag as a support can increase the concentration of CO near the Cu catalyst, which helps to further reduce CO_2 to C2-C3 products; thus, the highest (~45%) faradaic efficiency for C2 − C3 products was obtained by O_2 plasma-treated Cu/Ag catalyst, while, <30% of the Cu/Ag prepared by conventional electrodeposition. Gao et al. [28] compared the Cu nanocube catalyst treated with O_2 plasma to Ar and H_2 plasma and revealed that O_2 plasma-treated catalysts had more stable O^{2-} and some special defect sites. On the one hand, the electronic properties on the catalysts surface were changed by O_2 plasma treatment, on the other hand, the oxygen species produced can react with the surface adsorpted CO or intermediate product (COOH*), which are the key for achieving a high catalytic activity and hydrocarbon selectivity; thus, a maximum Faradaic efficiency (FE) of ~73% for C2 and C3 products was obtained in their study (Fig. 12a). A higher conversion was also found on the O_2 plasma-activated Ag catalyst for CO_2 electroreduction to CO. At −0.6 V versus RHE, >90% FE towards CO was achieved. The DFT calculations showed that in the presence of a local electric field, the highly defective surface produced by plasma oxidation could reduce the thermodynamic barrier and reduce CO_2 to CO under a low overpotential [124]. Furthermore, the presence of Cl^-, Br^- and I^- in the electrolyte can reduce the overpotential of the plasma pre-oxidation Cu catalyst without sacrificing its inherent high C_2-C_3 product selectivity and increase the rate of CO_2 electroreduction by providing a partial charge to CO_2, which promotes the adsorption of CO_2 and facilitates the formation and stabilization of the carboxyl (*COOH) intermediate, as shown in Fig. 12b [69].

CO_2 photocatalytic reduction is also an environmentally friendly and sustainable method that uses sunlight as an energy source to convert CO_2 into usable fuel or chemical raw materials [125]. For the Ag/TiO_2 catalyst, using atmospheric pressure DBD cold plasma as a reducing agent can achieve complete and rapid conversion of Ag^+ to Ag^0, improving the photocatalytic reduction of CO_2 under visible light and the highest CO and CH_4 production rates of approximately 72 μmol g^{-1} and 6.8 μmol g^{-1}, respectively. The LSPR caused by the small Ag NPs with high dispersion produced by NTP is the main reason, which not only helps the photogenerated electron-hole pairs in TiO_2 separate from the recombination, but also promotes the absorption of visible light to excite electrons on the catalyst surface, contributing to speeding up the reaction via the formation of some active intermediate products ($\cdot CO_2^-$, H^+, e.g.) (Fig. 13) [126]. A large number of Bi quantum dots (Bi QDs) were reduced in situ on the surface of black Bi_2WO_6 nanosheets using DBD plasma by Zhong et al. [127], thus promoting the generation of a large number of unsaturated coordination atoms. Due to the unique interface design, black Bi_2WO_6 showed an outstanding CO generation rate, which was approximately three times higher than that of the original Bi_2WO_6 nanosheets. In addition, the oxygen vacancy on the surface of the photocatalyst is one of the important factors for improving the performance of photocatalytic CO_2 reduction [128]. It was reported that Bi_2WO_6 ultrathin nanosheets with more oxygen vacancies introduced by NTP showed an excellent activity, and the CO production rate was 40.6 μmol g^{-1} h^{-1} in the CO_2 photocatalytic reduction (Fig. 14). The new level of defects caused by introducing oxygen vacancies makes the

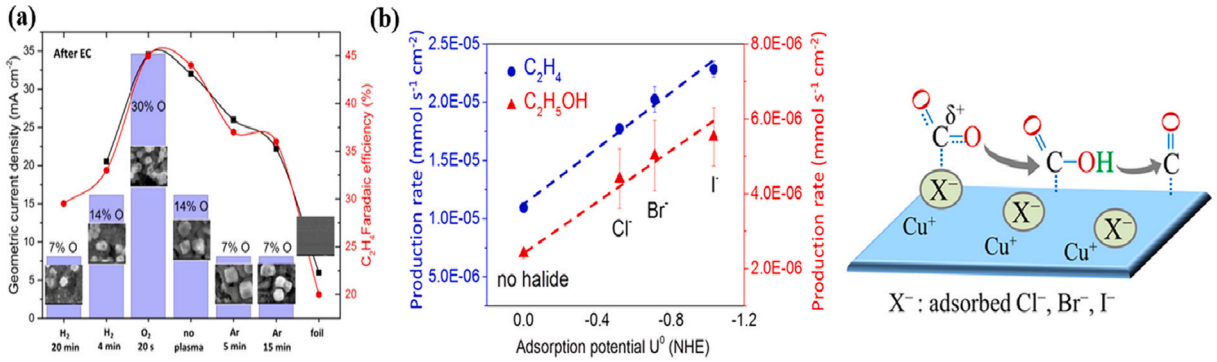

Fig. 12. (a) The oxygen content and SEM image of the cube under different modified conditions, and the corresponding geometric current density (left axis) and Faraday efficiency (right axis) of C_2H_4 [28], (b) Schematic diagram of how adsorbed halide promote CO_2 adsorption and degradation [69].

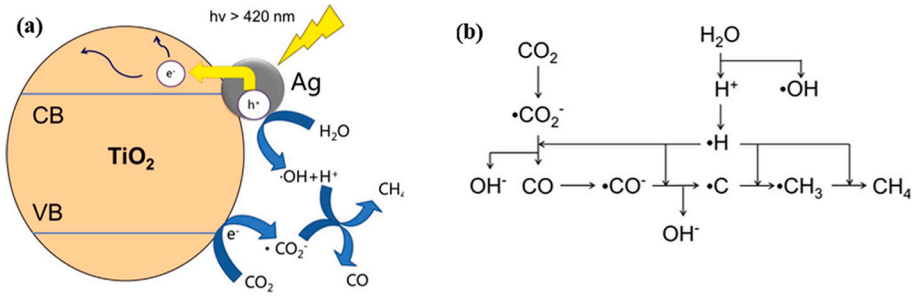

Fig. 13. Schematic diagram of (a) the enhancement mechanism of Ag NPs modified TiO_2 photocatalytic activity and (b) the corresponding gas phase photocatalytic reaction process [126].

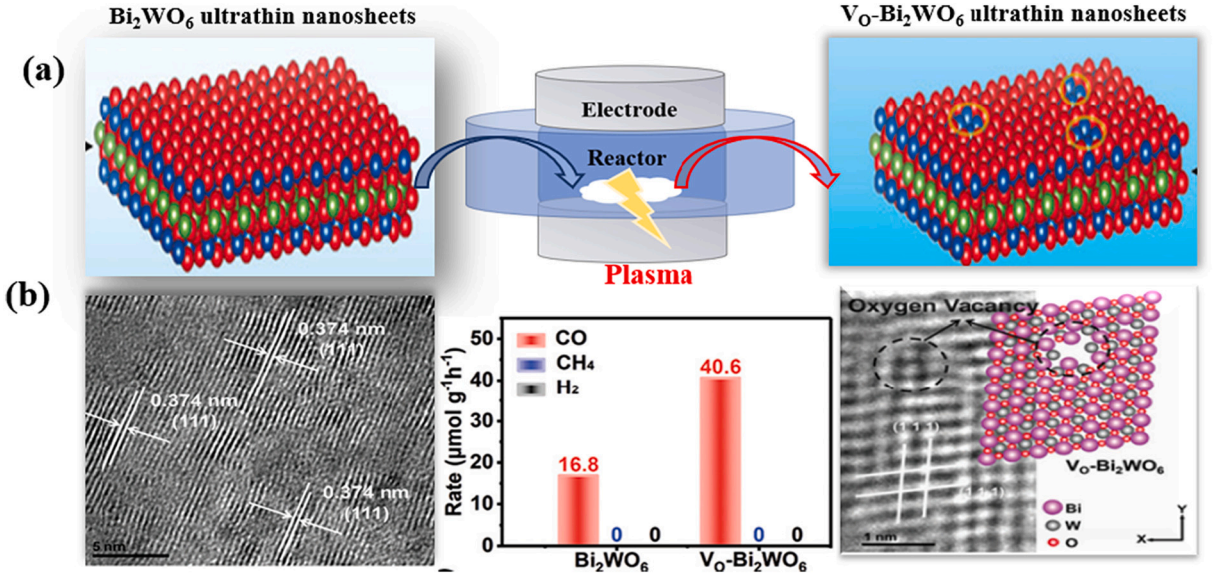

Fig. 14. (a) Modification schematic of Bi_2WO_6 ultra-thin nanosheet. (b) Corresponding HRTEM image and structure model and the product generation rate of Bi_2WO_6 and oxygen vacancy-Bi_2WO_6 (V_O-Bi_2WO_6) [129].

electrons more susceptible to light excitation and transfers to the conduction band and increases the light absorption [129].

CO_2 methanation is a type of CO_2 reduction reaction [130–132]. Ni/Ce/SBA-15 treated with DBD plasma not only have the highest activity for CO and CO_2 methanation at 450 °C (X_{CO2max} = 79.8%, $Y_{CH4} \approx$ 80%; $X_{COmax} \approx$ 97%, $Y_{CH4} \approx$ 90%, where X is the removal rate and Y is the yield) but also have a good high-temperature stability (decreased from 84.9% to 73.1%) at 650 °C for 30 h. Moreover, the TG analysis showed a lower carbon deposition amount in the NTP catalyst. Compared to the thermal calcination, the XRD pattern showed that no NiO diffraction signal was detected in the NTP prepared Ni/SBA-15, and the surface NiO particles size was significantly reduced (14.4 nm → 5.9 nm), which was evidenced by TEM, indicating that the NiO species were smaller and highly dispersed in the mesoporous skeleton [133]. Fan et al. [134] reported that Ni/$MgAl_2O_4$ prepared by DBD plasma could effectively improve the conversion efficiency of CO_2 to methane due to the smaller Ni particles and stronger metal-support interactions. The methane yield can reach 71.8% at 300 °C but only 62.9% using the heat treatment

catalyst. An FTIR analysis showed that the reaction pathway changed after DBD plasma treatment, following the mechanism via the CO intermediate, but the catalyst prepared by thermal decomposition adopts the direct hydrogenation of formate [16]. Interestingly, an appropriate Ni precursor and support have a synergistic effect with the unique low-temperature and high-energy characteristics of plasma technology. Xu et al. [135] used layered double hydroxides (LDHs) as the precursor to synthesize a Ni-Ce/Al_2O_3 catalyst (Ni-Ce-LDH-P) via NTP. LDHs enhanced the interactions between Ni—Al and Ni—Ce and improved the alkalinity of the catalyst, thereby increasing the low-temperature activity of the catalyst (200–350 °C), which can be further optimized by NTP. It was reported that Ni/CeO_2 is more active for CO and CO_2 methanation than other supported Ni catalysts due to its unique Ce-O-Ni interactions [136,137]. With the help of plasma, the catalyst exhibits a superior low-temperature activity at 250 °C, where the CO conversion rate was 96.8%, the methane selectivity was close to 100%, and the carbon resistance was also enhanced, while the CO conversion rate of the thermal treatment catalyst was only 14.7% [138].

3.2.2. *Hydrocarbon reforming*

Methane reforming is considered a potential method for converting methane and CO_2 (the two main greenhouse gases) into valuable hydrocarbons or gaseous fuels (H_2) [139]. Due to the ability to initiate chemical reactions at lower temperatures, glow discharge plasma can effectively reduce the metal particles on the support and improve their dispersion, thereby improving the anti-coke property and activity [26,140]. Rahimi et al. [141] used an Ar glow discharge plasma to prepare Ni/Al_2O_3–ZrO_2 nanocatalysts for CO_2 reforming of methane. In the nanocatalyst, the smooth Ni particles were found to be well distributed on the alumina support with a larger contact interface, which promotes the rate-determining step in the reaction mechanism (the reaction between NiC and Al_2O_4 on the interface). In addition, NTP also promoted the dispersion of ZrO_2, which effectively inhibited the deposition of coke. Due to oxygen adsorption, ZrO_2 (O-ZrO_2) reacts very quickly with carbon deposits. They also studied the effect of Ni-Co/Al_2O_3–ZrO_2 treated by glow discharge plasma with different voltages (700 V, 1000 V, and 1300 V) on CO_2 reforming of methane. When the voltage was higher than 1000 V, the energy efficiency of the plasma was reduced due to the energy loss caused by collisions between electrons and reactor walls.

The 1000 V-treated nanocatalyst exhibited a 99% feed conversion at 850 °C, the H_2/CO ratio was 0.98 and showed a good stability for 1440 min due to it having the best surface properties [142]. Guo et al. [143] found that the Mn promoter has a modifying effect on the alkalinity of the plasma-treated catalyst, which is beneficial for eliminating carbon deposits and improving the coking resistance. Moreover, hydrocarbon steam reforming has been widely used in industrial hydrogen production or synthesis gas [144]. Thermodynamically, when the ratio of steam to methane is lower than 1.4, it is easy to generate carbon [145]. Therefore, to prevent carbon deposition people often use higher reaction temperatures and excess steam, which not only consumes energy, but also leads to possible sintering of the active sites [146]. Zhang et al. [15] reported that a DBD plasma-treated catalyst can effectively inhibit the production of coke under an extremely low steam-to-methane ratio (H_2O/CH_4 = 0.5). As shown in the TEM image of Fig. 15, compared with Ni/SiO_2 treated by DBD plasma, the thermally calcined nickel shows a larger “dark spots”. This indicates that the plasma treatment optimizes the catalyst surface structure with smaller Ni particle size and higher dispersion, leading to a moderate decomposition rate of CH4, and further producing slower and less formation of C* on the metal surface, considering to C has more opportunities to react with active oxygen, which was beneficial for reaching a better balance between the carbon deposition and gasification, as seen from Fig. 15e. Compared with thermal calcination, the NTP-modified catalyst has less carbon deposition.

In addition to methane reforming, NTP modification can also significantly promote the steam reforming of nonmethane hydrocarbons. It was reported that H_2 plasma treatment was an effective way to improve the hydrogen production and durability of nickel catalysts. At 810 K, the ethanol conversion rate of the plasma-treated catalyst reached 96.2%, the carbon balance reached 97%, and the final hydrogen production reached 320 mg/h gcat, which was 10% higher than that of the untreated catalyst. H atoms dissociated by H_2 plasma reduced the NiO on the surface to Ni^0 with a small particle size and a high dispersion through collisions with metals. At the same time, the dissociated O atoms and H atoms generate hydroxyl groups or water via three-body collision by recombination, thereby promoting the hydrolysis of ethanol [147]. Wang et al. [148] found that NTP treatment instead of thermal calcination not only increased the H_2 selectivity of Ni/CeO_2 in the glycerol steam reforming reaction, but also inhibited the deposition of coke by forming Ni-O-Ce composite materials. Additionally, different nickel sources also affect the method of carbon deposition. The amount of carbon deposition and the formation rate of the catalyst prepared with nickel nitrate as the precursor were higher than those with nickel chloride as the precursor. In addition to the precursor, the preparation method and processing atmosphere will also affect the conversion efficiency of hydrocarbons. The combination of co-precipitation preparation and glow discharge plasma treatment can make the CuO (111) microcrystalline plate more dispersed, and the smaller Cu particles can effectively inhibit the direct decomposition of methanol into by-product CO and increase the H_2 selectivity (by approximately 80%) [149]. In the reaction of acetylene hydrogenation to ethylene, Jang et al. [150] found that using oxygen as a plasma source can enhance the interactions of metal and support. This catalyst can increase the selectivity of ethylene through a charge transfer, while treatment with Ar or H_2 can be more effective in reducing metal precursors and avoiding particle aggregation at high temperatures. In general, the acetylene conversion rate of plasma-treated samples was close to 100% at temperatures above 49 °C, while the conversion rate with heat treatment was lower than 90% [151,152].

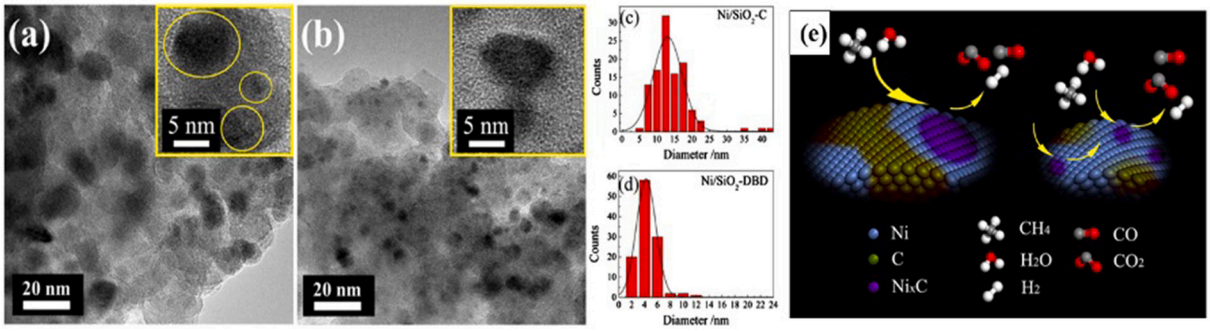

Fig. 15. TEM image and corresponding particle size distribution of (a) Ni/SiO_2-C and (b) Ni/SiO_2-DBD catalysts. (e) Schematic diagram of SRM reaction on Ni/SiO_2-C (left) and Ni/SiO_2-DBD (right) catalysts [15].

3.2.3. Electrochemical energy conversion and storage

The hydrogen evolution reaction (HER), oxygen evolution reaction (OER), and oxygen reduction reaction (ORR) are the most important reactions in the energy conversion and storage fields. Some noble metals (Pt, Ru, etc.) are recognized as the best electrocatalysts in this type of electrocatalytic reaction; however, the high prices and poor stability of noble metals limit their wide application.

Tao et al. [70] successfully prepared edge-rich graphene and CNTs with more edges/defects via Ar plasma etching, which presented an excellent ORR activity through one-step and four-electron pathways, and the ORR onset potentials were 0.912 V and 0.83 V, respectively. DFT showed that, compared with basal plane carbon, edge carbon has a higher charge density, which is most likely to be a catalytically active site. Jiang et al. [153] used microwave-induced plasma etching technology with different gas sources to improve the OER activity of a Co-MOF-74 catalyst. Catalysts treated with H_2 plasma showed the lowest overpotential (337 mV at 15 mA cm^{-2}), highest TOF (0.0219 s^{-1}), and largest mass activity (54.3 A g^{-1}) due to the exposure of more coordinatively unsaturated metal sites (the active sites of MOF catalysts) around the ligand vacancies. The catalysts prepared by Ar treatment presented a moderate improvement in terms of OER activity, which is attributed to partial active sites. However, during the CH_4 plasma treatment, CH_4 may decompose on the metal sites, causing carbon deposition to partially hinder the contact between the metal sites and the reactants. In addition, NTP can appropriately control the valence state of elements in the catalyst and change the electronic performance. Xu et al. [45] designed an efficient Co_3O_4-based OER electrocatalyst through the Ar RF plasma etching strategy with a higher surface area and oxygen vacancies on the Co_3O_4 surface, resulting in more Co^{2+} being formed, which was the active site for the OER and could promote the formation of cobalt oxyhydroxide (CoOOH) as the active site for the OER. Thus, etched Co_3O_4 has a higher current density and a lower starting potential.

Recent studies have shown that doping heteroatoms (N, B, S, P, F, Cl, etc.) into the carbon framework is an effective way to improve the catalytic performance of carbon-based materials. The spin density and charge distribution have changed [154,155]. Some scholars have also determined that the combination of traditional heteroatom doping technology and plasma-assisted defect engineering opens up a new pathway for the development of high-efficiency carbon-based catalysts. Tian et al. [46] used RF plasma to introduce defects on the surface of 3D nitrogen-doped graphene (3DNG) synthesized by the hydrothermal method. Among them, the 3D structure reduces the polarization resistance of the HER by providing an effective electron/ion transport pathway. N elements and plasma-induced defects are the active centres of HER. The synergistic effect of the 3D structure, N element doping and defects helps further enhance the HER activity and stability. Moreover, they also found similar results on plasma-etched, S-doped graphene catalysts [47]. Additionally, NTP can also directly introduce heteroatoms into the catalyst. For example, NH_3 and N_2 plasma can be used to introduce nitrogen into graphene-based catalysts to promote ORR, HER and OER activity [72,156,157]. Mohan [158] reported that O_2 plasma can dope O in single-walled carbon nanotubes (SWCNTs) and multi-walled carbon nanotubes (MWCNTs) to improve the wettability of the catalyst, resulting in the double-layer capacitance of two CNTs increasing to 1.32 and 1.6 times, respectively. O_2 plasma treatment can inhibit the formation of corrosive H_2O_2 or HO_2^- during the ORR reaction. Recently, Li et al. [159] realized tunable coordination of a single-atom catalyst Pt/C by changing the gas type (N_2, Ar or Air) and the treatment time of NTP. It is worth nothing that the sample of N, O co-dopant introduced by air plasma showed a higher TOF ~ 13 H_2 s^{-1} at 40 mV and an excellent mass activity of 7.41 A mg^{-1}_{Pt} for HER, which was 26.5 times that of a commercial Pt/C catalyst.

4. Conclusions and outlook

Nonthermal plasma, provides opportunities in surface modification and engineering new class of materials with target properties. Plasma, as an emerging fast-developing catalytic treatment technology, has attracted a lot of attention in last years in the scientific community and in industry. This review systematically summarized research performed in recent years, classified and explained the improved properties of catalysts after NTP treatment, and provided a comprehensive overview of the application of modified catalysts in the environmental and energy fields.

The approaches and technologies based on the use of NTP in the field of catalysts give researchers and engineers new tools for materials engineering which are unique and capable of synthesis novel surfaces and precisely controlled morphology and chemistry. The NTP advantages over other methods are:

(i) Compared to some conventional thermal or chemical methods, NTP can improve surface particle dispersion and particle size without changing the crystal structure of the catalyst itself, due to milder reaction conditions and higher reactivity.
(ii) NTP has been proven to control the surface morphology of the catalyst, such as the pore structure, roughness, and topography. The control over the material surface can be achieved on the micro (particles), nano-, molecular and even atomic scales that are distinguishable different from all other approaches used in the field.
(iii) Unfavourable thermodynamic reactions can be initiated by NTP treatment, assisting in the synthesis of various functional groups and optimizing the redox properties of catalysts with the help of reactive species, such as atomic oxygen and hydrogen.
(iv) Defects generated in the catalyst could anchor the metal onto the surface of the support. It can inhibit the aggregation of metal particles on the surface and thereby enhance the catalysts interaction with the support.
(v) For heat-sensitive processes, NTP provides the possibility of removing impurities, templates, and degradation of organic compounds during the synthesis.
(vi) Deactivation of catalysts caused by carbonaceous deposits can be reversed by NTP treatment withhigh efficiency in eliminating carbonaceous compounds under mild conditions. Although some report on the ability to remove other poisoned species by NTP, a deep investigation is needed to understand the process.
(vii) The application of NTP in the environmental field of VOC abatement, NOx and CO removal has shown the capability of plasma treatment to optimize catalysts oxygen vacancies, dispersion of active sites and morphology, helping pollutant decomposition. However, the exact mechanisms of plasma modification are mostly unknown and an in-situ experimental data are rare .
(viii) In the field of hydrocarbons reforming and CO_2 reduction, the improved electrochemical characteristics of catalysts can be achieved by NTP treatment that lowers the thermodynamic barrier, accelerating the CO_2 photoelectric reduction and can substantially improve the catalysts anti-coking performance. Due to the unique capabilities of plasma to control chemical modification of the surfaces, even on the atomic scale, the reducing/redox ability of catalysts can be tuned in a very wide range. This helps improving the electrical properties of catalysts, current density and the initial potential, which are the key features for energy conversion and catalysts storage capacity.

As shown in the current review Nonthermal plasma modification can provide several unique capabilities in controlling the catalytic performance and is an alternative to other modification approaches. Available results validate the positive effect of plasma treatment of different

catalysts. However, there are still many points to be addressed and challenges to be solved in the use of plasma technology:

(1) The NTP modification process is complicated and includes a combination of various disciplines, physics, thermodynamics, chemistry, and materials science. Unfortunately, there is still a lack of in-situ characterization techniques, making it difficult to analyse the modification process in a flash. Our future research should be directed to develop and adapt the methods of direct in-situ detection of plasma processes with high temporal and spatial resolution.
(2) The discharge conditions, such as the carrier gas, input energy, reactor configuration and threatment time, greatly affect the modification process. Full implementation of plasma treatment would require that these factors be deeply investigated and analysed. In addition, it is a priority to design an appropriate plasma reactor considering the requirement of uniform and stable discharge. Currently, the “test and try” approach is still mostly in use, which strongly limits progress in the field and requires more attention.
(3) Most of the applications of NTP-modified catalysts are still performed on a lab scale. More attention needs to be paid to solving the obstacles and challenges in industrial applications in order to improve the commercial feasibility of NTP-modified catalysts.

Based on the achievements of nonthermal plasma modification already acheived, it is expected that plasma technology will be even at higher demands in the near future. The unique ability of NTP to modify catalysts on different scales provides new opportunities in application fields, such as the preparation or modification of heat-sensitive substrates and various nanostructured catalysts. Therefore, incorporating the plasma modification method into the “real life” catalytic process and chemical technology is a subject of further exploration. In order to reach such an ambitious goal development of numerical methods or models that can predict the required plasma conditions is of high importance. Only a combination of numerical methods with experimental validation of the results and new characterization techniques can help to explore the “black box” mechanism of plasma and establish a new paradigm in the field of catalysts synthesis and materials engineering.

Declaration of Competing Interest

The authors declare that they have no known competing financial interests or personal relationships that could have appeared to influence the work reported in this paper.

Acknowledgments

The authors are thanks for the financial supports provided by the National Natural Science Foundation of China (22108255), China Postdoctoral Science Foundation (2022M712226) and State Environmental Protection Key Laboratory of Sources and Control of Air Pollution Complex (SCAPC202108).

References

[1] Giannakakis G, Flytzani-Stephanopoulos M, Sykes ECH, Tufts Univ MMA. Single-atom alloys as a reductionist approach to the rational design of heterogeneous catalysts. Acc Chem Res 2019;52:237–47.
[2] Cao J-L, Wang Y, Zhang T-Y, Wu S-H, Yuan Z-Y. Preparation, characterization and catalytic behavior of nanostructured mesoporous $CuO/Ce_{0.8}Zr_{0.2}O_2$ catalysts for low-temperature CO oxidation. Appl Catal B-Environ 2008;78:120–8.
[3] Karousis N, Tagmatarchis N, Tasis D. Current progress on the chemical modification of carbon nanotubes. Chem Rev 2010;110:5366–97.
[4] Queffelec C, Petit M, Janvier P, Knight DA, Bujoli B. Surface modification using phosphonic acids and esters. Chem Rev 2012;112:3777–807.
[5] Kusche M, Bustillo K, Agel F, Wasserscheid P. Highly effective Pt-based water-gas shift catalysts by surface modification with alkali hydroxide salts. ChemCatChem 2015;7:766–75.
[6] Sun Z, Sun B, Qiao M, Wei J, Yue Q, Wang C, et al. A general chelate-assisted co-assembly to metallic nanoparticles-incorporated ordered mesoporous carbon catalysts for fischer–tropsch synthesis. J Am Chem Soc 2012;134:17653–60.
[7] Bai B, Li J. Positive effects of K^+ ions on three-dimensional mesoporous Ag/Co_3O_4 catalyst for HCHO oxidation. ACS Catal 2014;4:2753–62.
[8] Zhang C, Liu F, Zhai Y, Ariga H, Yi N, Liu Y, et al. Alkali-metal-promoted Pt/TiO_2 opens a more efficient pathway to formaldehyde oxidation at ambient temperatures. Angew Chem Int Ed Engl 2012;51:9628–32.
[9] Martina K, Tagliapietra S, Barge A, Cravotto G. Combined microwaves/ultrasound, a hybrid technology. Top Curr Chem (Cham) 2016;374:79.
[10] Liang T, Qian J, Yuan Y, Liu C. Synthesis of mesoporous hydroxyapatite nanoparticles using a template-free sonochemistry-assisted microwave method. J Mater Chem 2013;48:5334–41.
[11] Hu Y, Li L, Zhang L, Lv Y. Dielectric barrier discharge plasma-assisted fabrication of g-C_3N_4 -Mn_3O_4 composite for high-performance cataluminescence H_2S gas sensor. Sens Actuator B-Chem 2017;239:1177–84.
[12] Wang Q, Wang X, Chai Z, Hu W. Low-temperature plasma synthesis of carbon nanotubes and graphene based materials and their fuel cell applications. Chem Soc Rev 2013;42:8821–34.
[13] Wang Z, Zhang Y, Neyts EC, Cao X, Zhang X, Jang BWL, et al. Catalyst preparation with plasmas: how does it work? ACS Catal 2018;8:2093–110.
[14] Yan X, Zhao B, Liu Y, Li Y. Dielectric barrier discharge plasma for preparation of Ni-based catalysts with enhanced coke resistance: current status andperspective. Catal Today 2015;256:29–40.
[15] Zhang Y, Wang W, Wang Z, Zhou X, Wang Z, Liu C-J. Steam reforming of methane over Ni/SiO_2 catalyst with enhanced coke resistance at low steam to methane ratio. Catal Today 2015;256:130–6.
[16] Zhou R, Rui N, Fan Z, Liu C-j. Effect of the structure of Ni/TiO_2 catalyst on CO_2 methanation. Int J Hydrogen Energy 2016;41:22017–25.
[17] Liu C, Li M, Wang J, Zhou X, Guo Q, Yan J, et al. Plasma methods for preparing green catalysts: current status and perspective. Chin J Catal 2016;37:340–8.
[18] Chu W, Xu J, Hong J, Lin T, Khodakov A. Design of efficient Fischer Tropsch cobalt catalysts via plasma enhancement: reducibility and performance (Review). Catal Today 2015;256:41–8.
[19] Liu H, Yang J, Qiao X, Jin Y, Fan B. Microwave plasma-assisted catalytic reduction of NO by active coke over transition-metal oxides. Energy Fuel 2020;34:4384–92.
[20] Mei D, Zhu X, Wu C, Ashford B, Williams PT, Tu X. Plasma-photocatalytic conversion of CO_2 at low temperatures: understanding the synergistic effect of plasma-catalysis. Appl Catal B-Environ 2016;182:525–32.
[21] Pan KL, He CB, Chang MB. Oxidation of TCE by combining perovskite-type catalyst with DBD. IEEE Trans Plasma Sci 2019;47:1152–63.
[22] Chung W-C, Chang M-B. Review of catalysis and plasma performance on dry reforming of CH_4 and possible synergistic effects. Renew Sustain Energy Rev 2016;62:13–31.
[23] Di L, Zhang J, Zhang X, Wang H, Li H, Li Y, et al. Cold plasma treatment of catalytic materials: a review. J Phys D Appl Phys 2021;54:333001.
[24] Liu C-j, Vissokov GP, Jang BWL. Catalyst preparation using plasma technologies. Catal Today 2002;72:173–84.
[25] Bharti B, Kumar S, Lee HN, Kumar R. Formation of oxygen vacancies and Ti(3+) state in TiO_2 thin film and enhanced optical properties by air plasma treatment. Sci Rep 2016;6:32355.
[26] Zhu X, Huo P, Zhang Y, Cheng D. Liu C-j. Structure and reactivity of plasma treated Ni/Al_2O_3 catalyst for CO_2 reforming of methane. Appl Catal B-Environ 2008;81:132–40.
[27] Ouyang B, Zhang Y, Wang Y, Zhang Z, Fan HJ, Rawat RS. Plasma surface functionalization induces nanostructuring and nitrogen-doping in carbon cloth with enhanced energy storage performance. J Mater Chem A 2016;4:17801–8.
[28] Gao D, Zegkinoglou I, Divins NJ, Scholten F, Sinev I, Grosse P, et al. Plasma-activated copper nanocube catalysts for efficient carbon dioxide electroreduction to hydrocarbons and alcohols. ACS Nano 2017;11:4825–31.
[29] Di L, Li Z, Park D-W, Lee B, Zhang X. Atmospheric-pressure cold plasma for synthesizing Pd/FeOx catalysts with enhanced low-temperature CO oxidation activity. Jpn J Appl Phys 2017;56:060301.
[30] Gao J, Zhu X, Bian Z, Jin T, Hu J, Liu H. Paving the way for surface modification in one-dimensional channels of mesoporous materials via plasma treatment. Microporous Mesoporous Mater 2015;202:16–21.
[31] Wang W, Wang Z, Wang J, Zhong CJ, Liu CJ. Highly active and stable Pt–Pd alloy catalysts synthesized by room-temperature electron reduction for oxygen reduction reaction. Adv Sci 2017;4. 1600486-n/a.
[32] Karuppiah J, Mok YS. Plasma-reduced $Ni/\gamma–Al_2O_3$ and $CeO_2–Ni/\gamma–Al_2O_3$ catalysts for improving dry reforming of propane. Int J Hydrogen Energy 2014;39:16329–38.
[33] Liu C-J, Zhao Y, Li Y, Zhang D-S, Chang Z, Bu X-H. Perspectives on electron-assisted reduction for preparation of highly dispersed noble metal catalysts. ACS Sustain Chem Eng 2013;2:3–13.
[34] Hong J, Du J, Wang B, Zhang Y, Liu C, Xiong H, et al. Plasma-assisted preparation of highly dispersed cobalt catalysts for enhanced fischer–tropsch synthesis performance. ACS Catal 2018;8:6177–85.
[35] Karuppiah J, Mok YS. Plasma-reduced $Ni/\gamma–Al_2O_3$ and $CeO_2–Ni/\gamma–Al_2O_3$ catalysts for improving dry reforming of propane. Int J Hydrogen Energy 2014;39:16329–38.
[36] Cao X, Zhou R, Rui N, Wang Z, Wang J, Zhou X, et al. Co_3O_4 /HZSM-5 catalysts for methane combustion: the effect of preparation methodologies. Catal Today 2017;297:219–27.

[37] Guo X, Sun Y, Yu Y, Zhu X, Liu C-J. Carbon formation and steam reforming of methane on silica supported nickel catalysts. Cat Com 2012;19:61–5.
[38] El-Roz M, Lakiss L, Telegeiev I, Lebedev OI, Bazin P, Vicente A, et al. High-visible-light photoactivity of plasma-promoted vanadium clusters on nanozeolites for partial photooxidation of methanol. ACS Appl Mater Interfaces 2017;9:17846–55.
[39] Guo Y, Gao X, Zhang C, Wu Y, Chang X, Wang T, et al. Plasma modification of a Ni based metal-organic framework for efficient hydrogen evolution. J Mater Chem A 2019;7:8129–35.
[40] Hájková P, Tišler Z. Atmospheric plasma treated hydrotalcite-type catalyst. Catal Lett 2017;147:374–82.
[41] Shi L, Zhou Y, Qi S, Smith KJ, Tan X, Yan J, et al. Pt catalysts supported on H_2 and O_2 plasma-treated Al_2O_3 for hydrogenation and dehydrogenation of the liquid organic hydrogen carrier pair dibenzyltoluene and perhydrodibenzyltoluene. ACS Catal 2020;10:10661–71.
[42] Deng X-Q, Zhu B, Li X-S, Liu J-L, Zhu X, Zhu A-M. Visible-light photocatalytic oxidation of CO over plasmonic Au/TiO_2: Unusual features of oxygen plasma activation. Appl Catal B-Environ 2016;188:48–55.
[43] Buitrago-Sierra R, García-Fernández MJ, Pastor-Blas MM, Sepúlveda-Escribano A. Environmentally friendly reduction of a platinum catalyst precursor supported on polypyrrole. Green Chem 2013;15:1981–90.
[44] Xiao Z, Wang Y, Huang Y-C, Wei Z, Dong C-L, Ma J, et al. Filling the oxygen vacancies in Co_3O_4 with phosphorus: an ultra-efficient electrocatalyst for overall water splitting. Energ Environ Sci 2017;10:2563–9.
[45] Xu L, Jiang Q, Xiao Z, Li X, Huo J, Wang S, et al. Plasma-engraved Co_3O_4 nanosheets with oxygen vacancies and high surface area for the oxygen evolution reaction. Angew Chem Int Ed 2016;55:5277–81.
[46] Tian Y, Ye Y, Wang X, Peng S, Wei Z, Zhang X, et al. Three-dimensional N-doped, plasma-etched graphene: highly active metal-free catalyst for hydrogen evolution reaction. Appl Catal A-Gen 2017;529:127–33.
[47] Tian Y, Wei Z, Wang X, Peng S, Zhang X. Plasma-etched, S-doped graphene for effective hydrogen evolution reaction. Int J Hydrogen Energy 2017;42:4184–92.
[48] Santhosh M, Filipič G, Kovacevic E, Jagodar A, Berndt J, Strunskus T, et al. N-graphene nanowalls via plasma nitrogen incorporation and substitution: the experimental evidence. Nano-micro Lett. 2020;12:1–7. https://doi.org/10.1007/s40820-020-0395-5.
[49] Zhang L, Liu X, Scurrell MS. Cold plasmas in the modification of catalysts. Rev Chem Eng 2018;34:201–13.
[50] Li K, Tang X, Yi H, Ning P, Xiang Y, Wang J, et al. Research on manganese oxide catalysts surface pretreated with non-thermal plasma for NO catalytic oxidation capacity enhancement. Appl Surf Sci 2013;264:557–62.
[51] Liu L, Deng Q-F, Liu Y-P, Ren T-Z, Yuan Z-Y. HNO_3-activated mesoporous carbon catalyst for direct dehydrogenation of propane to propylene. Cat Com 2011;16:81–5.
[52] Liu L, Deng Q-F, Ma T-Y, Lin X-Z, Hou X-X, Liu Y-P, et al. Ordered mesoporous carbons: citric acid-catalyzed synthesis, nitrogen doping and CO_2 capture. J Mater Chem 2011;21:16001.
[53] Kang S, He M, Chen M, Liu Y, Wang Y, Wang Y, et al. Surface amino group regulation and structural engineering of graphitic carbon nitride with enhanced photocatalytic activity by ultrafast ammonia plasma immersion modification. ACS Appl Mater Interf. 2019;11:14952–9.
[54] Zhang M, Zhu X, Liang X, Wang Z. Preparation of highly efficient Au/C catalysts for glucose oxidation via novel plasma reduction. Cat Com 2012;25:92–5.
[55] Zhang S, Li X-S, Zhu B, Liu J-L, Zhu X, Zhu A-M, et al. Atmospheric-pressure O_2 plasma treatment of Au/TiO_2 catalysts for CO oxidation. Catal Today 2015;256:142–7.
[56] Loganathan K, Bose D, Weinkauf D. Surface modification of carbon black by nitrogen and allylamine plasma treatment for fuel cell electrocatalyst. Int J Hydrogen Energy 2014;39:15766–71.
[57] Ding D, Song Z-L, Cheng Z-Q, Liu W-N, Nie X-K, Bian X, et al. Plasma-assisted nitrogen doping of graphene-encapsulated Pt nanocrystals as efficient fuel cell catalysts. J Mater Chem A 2014;2:472–7.
[58] Dameron AA, Pylypenko S, Bult JB, Neyerlin KC, Engtrakul C, Bochert C, et al. Aligned carbon nanotube array functionalization for enhanced atomic layer deposition of platinum electrocatalysts. Appl Surf Sci 2012;258:5212–21.
[59] Shioyama H, Honjo K, Kiuchi M, Yamada Y, Ueda A, Kuriyama N, et al. C_2F_6 plasma treatment of a carbon support for a PEM fuel cell electrocatalyst. J Power Sources 2006;161:836–8.
[60] Liu Z, Zhao Z, Wang Y, Dou S, Yan D, Liu D, et al. In situ exfoliated, edge-rich, oxygen-functionalized graphene from carbon fibers for oxygen electrocatalysis. Adv Mater 2017:29.
[61] Wang Y, Craven M, Yu X, Ding J, Bryant P, Huang J, et al. Plasma-enhanced catalytic synthesis of ammonia over a Ni/Al_2O_3 catalyst at near-room temperature: insights into the importance of the catalyst surface on the reaction mechanism. ACS Catal 2019;9:10780–93.
[62] Shah J, Wang W, Bogaerts A, Carreon ML. Ammonia synthesis by radio frequency plasma catalysis: revealing the underlying mechanisms. ACS Appl Energ Mater 2018;1:4824–39.
[63] Wang Z-j, Liu Y, Shi P, Liu C-j, Liu Y. Al-MCM-41 supported palladium catalyst for methane combustion: Effect of the preparation methodologies. Appl Catal B-Environ 2009;90:570–7.
[64] Hu P, Huang Z, Amghouz Z, Makkee M, Xu F, Kapteijn F, et al. Electronic metal-support interactions in single-atom catalysts. Angew Chem Int Ed Engl 2014;53:3418–21.
[65] Brault P, Caillard A, Baranton S, Mougenot M, Cuynet S, Coutanceau C. One-step synthesis and chemical characterization of Pt-C nanowire composites by plasma sputtering. ChemSusChem 2013;6:1168–71.
[66] Liu L, Zhang H, Jia J, Sun T, Sun M. Direct molten polymerization synthesis of highly active samarium manganese perovskites with different morphologies for VOC removal. Inorg Chem 2018;57:8451–7.
[67] Pastor-Pérez L, Belda-Alcázar V, Marini C, Pastor-Blas MM, Sepúlveda-Escribano A, Ramos-Fernandez EV. Effect of cold Ar plasma treatment on the catalytic performance of Pt/CeO_2 in water-gas shift reaction (WGS). Appl Catal B-Environ 2018;225:121–7.
[68] Benrabbah R, Cavaniol C, Liu H, Ognier S, Cavadias S, Gálvez ME, et al. Plasma DBD activated ceria-zirconia-promoted Ni-catalysts for plasma catalytic CO_2 hydrogenation at low temperature. Cat Com 2017;89:73–6.
[69] Gao D, Scholten F, Roldan Cuenya B. Improved CO_2 electroreduction performance on plasma-activated Cu catalysts via electrolyte design: halide effect. ACS Catal 2017;7:5112–20.
[70] Tao L, Wang Q, Dou S, Ma Z, Huo J, Wang S, et al. Edge-rich and dopant-free graphene as a highly efficient metal-free electrocatalyst for the oxygen reduction reaction. Chem Commun 2016;52:2764–7.
[71] Ouyang B, Zhang Y, Zhang Z, Fan HJ, Rawat RS. Nitrogen-plasma-activated hierarchical nickel nitride nanocorals for energy applications. Small 2017:13.
[72] Dou S, Tao L, Huo J, Wang S, Dai L. Etched and doped Co_9S_8/graphene hybrid for oxygen electrocatalysis. Energ Environ Sci 2016;9:1320–6.
[73] Xu H, He C, Lin L, Shen J, Shang S. Direct formation of carbon supported Pt nanoparticles by plasma-based technique. Mater Lett 2019;255:126532.
[74] Tripathi N, Islam SS. A new approach for orientation-controlled growth of CNTs: an in-depth analysis on the role of oxygen plasma treatment to catalyst. Appl Nanosci 2017;7:125–9.
[75] Yang J, Esconjauregui S, Xie R, Sugime H, Makaryan T, D'Arsié L, et al. Effect of oxygen plasma alumina treatment on growth of carbon nanotube forests. J Phys Chem C 2014;118:18683–92.
[76] Moafi HF, Hafezi M, Khorram S, Zanjanchi MA. The effects of non-thermal plasma on the morphology of Ce-doped ZnO: synthesis, characterization and photocatalytic activity of hierarchical nanostructures. Plasma Chem Plasma Process 2016;37:159–76.
[77] Ajayan PM, Ajayan PM, Stephan O, Stephan O, Redlich P, Redlich P, et al. Carbon nanotubes as removable templates for metal oxide nanocomposites and nanostructures. Nature 1995;375:564–7.
[78] Yang S, Lei Y. Recent progress on surface pattern fabrications based on monolayer colloidal crystal templates and related applications. Nanoscale 2011;3:2768–82.
[79] Zhou M, Bao J, Xu Y, Zhang J, Xie J, Guan M, et al. Photoelectrodes based upon Mo:$BiVO_4$ inverse opals for photoelectrochemical water splitting. ACS Nano 2014;8:7088–98.
[80] Koczkur KM, Mourdikoudis S, Polavarapu L, Skrabalak SE. Polyvinylpyrrolidone (PVP) in nanoparticle synthesis. Dalton Trans 2015;44:17883–905.
[81] Xie Y, Kocaefe D, Chen C, Kocaefe Y. Review of research on template methods in preparation of nanomaterials. J Nanomater 2016;2016:1–10.
[82] Gehl B, Frömsdorf A, Aleksandrovic V, Schmidt T, Pretorius A, Flege J-I, et al. Structural and chemical effects of plasma treatment on close-packed colloidal nanoparticle layers. Adv Funct Mater 2008;18:2398–410.
[83] Reid B, Taylor A, Alvarez-Fernandez A, Ismael MH, Sharma S, Schmidt-Hansberg B, et al. Photocatalytic template removal by non-ozone-generating UV irradiation for the fabrication of well-defined mesoporous inorganic coatings. ACS Appl Mater Interfaces 2019;11:19308–14.
[84] Tarish S, Wang Z, Al-Haddad A, Wang C, Ispas A, Romanus H, et al. Synchronous formation of ZnO/ZnS core/Shell nanotube arrays with removal of template for meliorating photoelectronic performance. J Phys Chem C 2015;119:1575–82.
[85] Aumond T, Pinard L, Batiot-Dupeyrat C, Sachse A. Non-thermal plasma: a fast and efficient template removal approach allowing for new insights to the SBA-15 structure. Microporous Mesoporous Mater 2020;296:110015.
[86] Guo Q, With P, Liu Y, Gläser R, Liu C-J. Carbon template removal by dielectric-barrier discharge plasma for the preparation of zirconia. Catal Today 2013;211:156–61.
[87] Liu Y, Wang Z, Liu C-J. Mechanism of template removal for the synthesis of molecular sieves using dielectric barrier discharge. Catal Today 2015;256:137–41.
[88] Hu M, Zhao B, Zhao D-Y, Yuan M-T, Chen H, Hao Q-Q, et al. Effect of template removal using plasma treatment on the structure and catalytic performance of MCM-22. RSC Adv 2018;8:15372–9.
[89] El Roz M, Lakiss L, Valtchev V, Mintova S, Thibault-Starzyk F. Cold plasma as environmentally benign approach for activation of zeolite nanocrystals. Microporous Mesoporous Mater 2012;158:148–54.
[90] Shaw S, Tian X, Silva TF, Bobbitt JM, Naab F, Rodrigues CL, et al. Selective removal of ligands from colloidal nanocrystal assemblies with non-oxidizing he plasmas. Chem Mater 2018;30:5961–7.
[91] Zhong W, Chen J, Zhang P, Deng L, Yao L, Ren X, et al. Air plasma etching towards rich active sites in Fe/N-porous carbon for the oxygen reduction reaction with superior catalytic performance. J Mater Chem A 2017;5:16605–10.
[92] Ferrah D, Renault O, Marinov D, Arias-Zapata J, Chevalier N, Mariolle D, et al. CF_4/H_2 plasma cleaning of graphene regenerates electronic properties of the pristine material. ACS Applied Nano Mater. 2019;2:1356–66.
[93] Duprez D, DeMicheli MC, Marecot P, Barbier J, Ferretti OA, Ponzi EN. Deactivation of steam-reforming model catalysts by coke formation: I. kinetics of the formation of filamentous carbon in the hydrogenolysis of cyclopentane on Ni/Al_2O_3 catalysts. J Catal 1990;124:324–35.
[94] Trimm DL. Catalysts for the control of coking during steam reforming. Catal Today 1999;49:3–10.

[95] Hansen TW, DeLaRiva AT, Challa SR, Datye AK. Sintering of catalytic nanoparticles: particle migration or ostwald ripening? Acc Chem Res 2013;46:1720–30.

[96] Brandenberger S, Kröcher O, Casapu M, Tissler A, Althoff R. Hydrothermal deactivation of Fe-ZSM-5 catalysts for the selective catalytic reduction of NO with NH_3. Appl Catal B-Environ 2011;101:649–59.

[97] Lokteva ES, Lazhko AE, Golubina EV, Timofeev VV, Naumkin AV, Yagodovskaya TV, et al. Regeneration of Pd/TiO_2 catalyst deactivated in reductive CCl_4 transformations by the treatment with supercritical CO_2, ozone in supercritical CO_2 or oxygen plasma. J Supercrit Fluids 2011;58:263–71.

[98] Fan H-Y, Shi C, Li X-S, Zhang S, Liu J-L, Zhu A-M. In-situ plasma regeneration of deactivated Au/TiO_2 nanocatalysts during CO oxidation and effect of N_2 content. Appl Catal B-Environ 2012;119–120:49–55.

[99] Zhu B, Li X-S, Liu J-L, Liu J-B, Zhu X, Zhu A-M. In-situ regeneration of Au nanocatalysts by atmospheric-pressure air plasma: Significant contribution of water vapor. Appl Catal B-Environ 2015;179:69–77.

[100] Nikiforov AY, Sarani A, Leys C. The influence of water vapor content on electrical and spectral properties of an atmospheric pressure plasma jet. Plasma Sources Sci Technol 2011;20:015014.

[101] Zhou W, Ye Z, Nikiforov A, Chen J, Wang J, Zhao L, et al. The influence of relative humidity on double dielectric barrier discharge plasma for chlorobenzene removal. J Clean Prod 2021;288:125502.

[102] Ojeda M, Zhan B-Z, Iglesia E. Mechanistic interpretation of CO oxidation turnover rates on supported Au clusters. J Catal 2012;285:92–102.

[103] Zhu B, Liu J-L, Li X-S, Liu J-B, Zhu X, Zhu A-M. In situ regeneration of Au nanocatalysts by atmospheric-pressure air plasma: regeneration characteristics of square-wave pulsed plasma. Top Catal 2017;60:914–24.

[104] Kim T, Lee DH, Jo S, Pyun SH, Kim K-T, Song Y-H. Mechanism of the accelerated reduction of an oxidized metal catalyst under electric discharge. ChemCatChem 2016;8:685–9.

[105] AlQahtani MS, Wang X, Gray JL, Knecht SD, Bilén SG, Song C. Plasma-assisted catalytic reduction of SO_2 to elemental sulfur: Influence of nonthermal plasma and temperature on iron sulfide catalyst. J Catal 2020;391:260–72.

[106] Jia LY, Farouha A, Pinard L, Hedan S, Comparot JD, Dufour A, et al. New routes for complete regeneration of coked zeolite. Appl Catal B-Environ 2017;219:82–91.

[107] Li X-S, Ma X-Y, Liu J-L, Sun Z-G, Zhu B, Zhu A-M. Plasma-promoted Au/TiO_2 nanocatalysts for photocatalytic formaldehyde oxidation under visible-light irradiation. Catal Today 2019;337:132–8.

[108] Deng X-Q, Liu J-L, Li X-S, Zhu B, Zhu X, Zhu A-M. Kinetic study on visible-light photocatalytic removal of formaldehyde from air over plasmonic Au/TiO_2. Catal Today 2017;281:630–5.

[109] Wang B, Chen B, Sun Y, Xiao H, Xu X, Fu M, et al. Effects of dielectric barrier discharge plasma on the catalytic activity of Pt/CeO_2 catalysts. Appl Catal B-Environ 2018;238:328–38.

[110] Fu Y, Zhang Y, Xin Q, Zheng Z, Zhang Y, Yang Y, et al. Non-thermal plasma-modified Ru-Sn-Ti catalyst for chlorinated volatile organic compound degradation. Catalysts 2020;10:1456.

[111] Paolucci C, Khurana I, Parekh AA, Li S, Shih AJ, Li H, et al. Dynamic multinuclear sites formed by mobilized copper ions in NOx selective catalytic reduction. Science 2017;357:898–903.

[112] Han L, Cai S, Gao M, Hasegawa JY, Wang P, Zhang J, et al. Selective catalytic reduction of NOx with NH_3 by using novel catalysts: state of the art and future prospects. Chem Rev 2019;119:10916–76.

[113] Tang X, Gao F, Xiang Y, Yi H, Zhao S. Low temperature catalytic oxidation of nitric oxide over the Mn–CoOx catalyst modified by nonthermal plasma. Cat Com 2015;64:12–7.

[114] Zhang L, Wen X, Zhang L, Sha X, Wang Y, Chen J, et al. Study on the preparation of plasma-modified fly ash catalyst and its De(−)NOX mechanism. Materials (Basel) 2018;11.

[115] Liu L, Zheng C, Wu S, Gao X, Ni M, Cen K. Manganese-cerium oxide catalysts prepared by non-thermal plasma for NO oxidation: effect of O_2 in discharge atmosphere. Appl Surf Sci 2017;416:78–85.

[116] Liu Z, Yu F, Ma C, Dan J, Luo J, Dai B. A critical review of recent progress and perspective in practical denitration application. Catalysts 2019;9:771.

[117] Zhang H, Li K, Li L, Liu L, Meng X, Sun T, et al. High efficient styrene mineralization through novel $NiO\text{-}TiO_2\text{-}Al_2O_3$ packed pre-treatment/treatment/post-treatment dielectric barrier discharge plasma. Chem Eng J 2018;343:759–69.

[118] Huang H, Ye D, Huang B, Wei Z. Vanadium supported on viscose-based activated carbon fibers modified by oxygen plasma for the SCR of NO. Catal Today 2008;139:100–8.

[119] Nazarpoor Z, Ma S, Fanson PT, Alexeev OS, Amiridis MD. O_2 plasma activation of dendrimer-derived $Pt/\gamma\text{-}Al_2O_3$ catalysts. J Catal 2012;290:26–36.

[120] Zhang X, Xu W, Duan D, Park D-W, Di L. Atmospheric pressure oxygen cold plasma for synthesizing Au/TiO_2 catalysts: effect of discharge voltage and discharge time. IEEE Trans Plasma Sci 2018;46:2776–81.

[121] Qi B, Di L, Xu W, Zhang X. Dry plasma reduction to prepare a high performance Pd/C catalyst at atmospheric pressure for CO oxidation. J Mater Chem A 2014;2:11885.

[122] Mistry H, Varela AS, Bonifacio CS, Zegkinoglou I, Sinev I, Choi YW, et al. Highly selective plasma-activated copper catalysts for carbon dioxide reduction to ethylene. Nat Commun 2016;7:12123.

[123] Scholten F, Sinev I, Bernal M, Roldan Cuenya B. Plasma-modified dendritic Cu catalyst for CO_2 electroreduction. ACS Catal 2019;9:5496–502.

[124] Mistry H, Choi Y-W, Bagger A, Scholten F, Bonifacio CS, Sinev I, et al. Enhanced carbon dioxide electroreduction to carbon monoxide over defect-rich plasma-activated silver catalysts. Angew Chem Int Ed 2017;56:11394–8.

[125] Xu Y, Jia Y, Zhang Y, Nie R, Zhu Z, Wang J, et al. Photoelectrocatalytic reduction of CO_2 to methanol over the multi-functionalized TiO_2 photocathodes. Appl Catal B-Environ 2017;205:254–61.

[126] Cheng X, Dong P, Huang Z, Zhang Y, Chen Y, Nie X, et al. Green synthesis of plasmonic Ag nanoparticles anchored TiO_2 nanorod arrays using cold plasma for visible-light-driven photocatalytic reduction of CO_2. J CO_2 Util 2017;20:200–7.

[127] Zhong K, Zhou A, Zhou G, Li Q, Yang J, Wang Z, et al. Plasma-induced black bismuth tungstate as a photon harvester for photocatalytic carbon dioxide conversion. New J Chem 2021;45:1993–2000.

[128] Li J-h, Ren J, Liu Y, Mu H-y, Liu R-h, Zhao J, et al. In situ synthesis of Cl-doped $Bi_2O_2CO_3$ and its enhancement of photocatalytic activity by inducing generation of oxygen vacancies. Inorg Chem Front 2020;7:2969–78.

[129] Li Q, Zhu X, Yang J, Yu Q, Zhu X, Chu J, et al. Plasma treated Bi_2WO_6 ultrathin nanosheets with oxygen vacancies for improved photocatalytic CO_2 reduction. Inorg Chem Front 2020;7:597–602.

[130] Rönsch S, Schneider J, Matthischke S, Schlüter M, Götz M, Lefebvre J, et al. Review on methanation – from fundamentals to current projects. Fuel (Guildford) 2016;166:276–96.

[131] Jia X, Rui N, Zhang X, Hu X. Liu C-j. Ni/ZrO_2 by dielectric barrier discharge plasma decomposition with improved activity and enhanced coke resistance for CO methanation. Catal Today 2019;334:215–22.

[132] Jia X, Zhang X, Rui N, Hu X. Liu C-j. Structural effect of Ni/ZrO_2 catalyst on CO_2 methanation with enhanced activity. Appl Catal B-Environ 2019;244:159–69.

[133] Bian L, Zhang L, Zhu Z, Li Z. Methanation of carbon oxides on Ni/Ce/SBA-15 pretreated with dielectric barrier discharge plasma. Mol Catal 2018;446:131–9.

[134] Fan Z, Sun K, Rui N, Zhao B, Liu C. Improved activity of $Ni/MgAl_2O_4$ for CO_2 methanation by the plasma decomposition. J Energy Chem 2015;24:655–9.

[135] Xu Y, Chen Y, Li J, Zhou J, Song M, Zhang X, et al. Improved low-temperature activity of $Ni\text{–}Ce/\gamma\text{-}Al_2O_3$ catalyst with layer structural precursor prepared by cold plasma for CO_2 methanation. Int J Hydrogen Energy 2017;42:13085–91.

[136] Nematollahi B, Rezaei M, Lay EN. Selective methanation of carbon monoxide in hydrogen rich stream over Ni/CeO_2 nanocatalysts. J. Rare Earths 2015;33:619–28.

[137] Fukuhara C, Hayakawa K, Suzuki Y, Kawasaki W, Watanabe R. A novel nickel-based structured catalyst for CO_2 methanation: a honeycomb-type Ni/CeO_2 catalyst to transform greenhouse gas into useful resources. Appl Catal A-Gen 2017;532:12–8.

[138] Zhang X, Rui N, Jia X, Hu X. Liu C-j. Effect of decomposition of catalyst precursor on Ni/CeO_2 activity for CO methanation. Chin J Catal 2019;40:495–503.

[139] Rahemi N, Haghighi M, Babaluo AA, Allahyari S, Jafari MF. Syngas production from reforming of greenhouse gases CH_4/CO_2 over $Ni\text{–}Cu/Al_2O_3$ nanocatalyst: impregnated vs. plasma-treated catalyst. Energ Conver Manage 2014;84:50–9.

[140] Zhao Y, Pan Y-x, Xie Y, Liu C-j. Carbon dioxide reforming of methane over glow discharge plasma-reduced Ir/Al_2O_3 catalyst. Cat Com 2008;9:1558–62.

[141] Rahemi N, Haghighi M, Babaluo AA, Jafari MF, Estifaee P. Synthesis and physicochemical characterizations of $Ni/Al_2O_3\text{–}ZrO_2$ nanocatalyst prepared via impregnation method and treated with non-thermal plasma for CO_2 reforming of CH_4. J Ind Eng Chem 2013;19:1566–76.

[142] Rahemi N, Haghighi M, Babaluo AA, Allahyari S, Estifaee P, Jafari MF. Plasma-assisted dispersion of bimetallic Ni–Co over $Al_2O_3\text{–}ZrO_2$ for CO_2 reforming of methane: influence of voltage on catalytic properties. Top Catal 2017;60:843–54.

[143] Guo F, Xu J-Q, Chu W. CO_2 reforming of methane over Mn promoted Ni/Al_2O_3 catalyst treated by N_2 glow discharge plasma. Catal Today 2015;256:124–9.

[144] Nozaki T, Okazaki K. Non-thermal plasma catalysis of methane: principles, energy efficiency, and applications. Catal Today 2013;211:29–38.

[145] Van Hook JP. Methane-steam reforming. Catal Rev 1980;21:1–51.

[146] Bej B, Pradhan NC, Neogi S. Production of hydrogen by steam reforming of methane over alumina supported nano-NiO/SiO_2 catalyst. Catal Today 2013;207:28–35.

[147] Wu Y-W, Chung W-C, Chang M-B. Modification of $Ni/\gamma\text{-}Al_2O_3$ catalyst with plasma for steam reforming of ethanol to generate hydrogen. Int J Hydrogen Energy 2015;40:8071–80.

[148] Wang B, Xiong Y, Han Y, Hong J, Zhang Y, Li J, et al. Preparation of stable and highly active Ni/CeO_2 catalysts by glow discharge plasma technique for glycerol steam reforming. Appl Catal B-Environ 2019;249:257–65.

[149] Bagherzadeh SB, Haghighi M. Plasma-enhanced comparative hydrothermal and coprecipitation preparation of $CuO/ZnO/Al_2O_3$ nanocatalyst used in hydrogen production via methanol steam reforming. Energ Conver Manage 2017;142:452–65.

[150] Li Y, Jang BWL. Non-thermal RF plasma effects on surface properties of Pd/TiO_2 catalysts for selective hydrogenation of acetylene. Appl Catal A-Gen 2011;392:173–9.

[151] Li Y, Jang BWL. Selective hydrogenation of acetylene over Pd/Al_2O_3 catalysts: effect of non-thermal RF plasma preparation methodologies. Top Catal 2017;60:997–1008.

[152] Zhang S, Chen C-Y, Jang BWL, Zhu A-M. Radio-frequency H_2 plasma treatment of $AuPd/TiO_2$ catalyst for selective hydrogenation of acetylene in excess ethylene. Catal Today 2015;256:161–9.

[153] Jiang Z, Ge L, Zhuang L, Li M, Wang Z, Zhu Z. Fine-tuning the coordinatively unsaturated metal sites of metal–organic frameworks by plasma engraving for enhanced electrocatalytic activity. ACS Appl Mater Interfaces 2019;11:44300–7.

[154] Gao K, Wang B, Tao L, Cunning BV, Zhang Z, Wang S, et al. Efficient metal-free electrocatalysts from N-doped carbon nanomaterials: mono-doping and co-doping. Adv Mater 2019;31:e1805121.
[155] Lin T, Chen IW, Liu F, Yang C, Bi H, Xu F, et al. Nitrogen-doped mesoporous carbon of extraordinary capacitance for electrochemical energy storage. Science 2015;350:1508–13.
[156] Zhang Y, Ouyang B, Xu J, Chen S, Rawat RS, Fan HJ. 3D porous hierarchical nickel-molybdenum nitrides synthesized by RF plasma as highly active and stable hydrogen-evolution-reaction electrocatalysts. Adv Energy Mater 2016;6:1600221.
[157] Zhang Y, Ouyang B, Xu J, Jia G, Chen S, Rawat RS, et al. Rapid synthesis of cobalt nitride nanowires: highly efficient and low-cost catalysts for oxygen evolution. Angew Chem Int Ed Engl 2016;55:8670–4.
[158] Mohan R, Modak A, Schechter A. A comparative study of plasma-treated oxygen-doped single-walled and multiwalled carbon nanotubes as electrocatalyst for efficient oxygen reduction reaction. ACS Sustain Chem Eng 2019;7:11396–406.
[159] Li J, Zhou Y, Tang W, Zheng J, Gao X, Wang N, et al. Cold-plasma technique enabled supported Pt single atoms with tunable coordination for hydrogen evolution reaction. Appl Catal B-Environ 2021;285:119861.
[160] Chen B, Wang B, Sun Y, Wang X, Fu M, Wu J, et al. Plasma-assisted surface interactions of Pt/CeO_2 catalyst for enhanced toluene catalytic oxidation. Catalysts 2018;9:2.
[161] Wang H, Zhang Y, Wu M, Xu H, Jin X, Zhou J, et al. Pd/SiO_2 catalysts prepared via a dielectric barrier discharge hydrogen plasma with improved performance for low-temperature catalytic combustion of toluene. Ind Eng Chem Res 2020;59:20316–24.
[162] Khaledian HR, Zolfaghari P, Nezhad PDK, Niaei A, Khorram S, Salari D. Surface modification of $LaMnO_3$ perovskite supported on CeO_2 using argon plasma for high-performance reduction of NO. J Environ Chem Eng 2021;9:104581.
[163] Li Y, Jang BWL. Selective hydrogenation of acetylene over Pd/Al_2O_3 catalysts: effect of non-thermal RF plasma preparation methodologies. Top Catal 2017;60:997–1008.
[164] Fan Z, Sun K, Rui N, Zhao B, Liu C-J. Improved activity of Ni/$MgAl_2O_4$ for CO_2 methanation by the plasma decomposition. J Energy Chem 2015;24:655–9.
[165] Zhao B, Yao Y, Shi H, Yang F, Jia X, Liu P, et al. Preparation of Ni/SiO_2 catalyst via novel plasma-induced micro-combustion method. Catal Today 2019;337:28–36.
[166] Lian J, Fang X, Liu W, Huang Q, Sun Q, Wang H, et al. Ni supported on $LaFeO_3$ perovskites for methane steam reforming: on the promotional effects of plasma treatment in H_2–Ar atmosphere. Top Catal 2017;60:831–42.